U.S. Geological Survey Final Technical Report

Award No. G16AP00100
Recipient: University of California at Santa Barbara

An Integrated Onshore-Offshore Re-Evaluation of 3D Fault and Fold Geometry, Coastal Uplift and Seismic Hazard in the Santa Barbara-Ventura Area

Craig Nicholson[1], Christopher Sorlien[2], Marc J. Kamerling[3]
& Thomas E. Hopps[4]
[1]*Marine Science Institute, University of California, Santa Barbara, CA*
[2]*Earth Research Institute, University of California, Santa Barbara, CA*
[3]*Geoscience Consultant, Santa Barbara, CA*
[4]*Rancho Energy Consultants, Inc., Ventura, CA*

Principal Investigator: Craig Nicholson
Marine Science Institute, University of California
MC 6150, Santa Barbara, CA 93106-6150
phone: 805-893-8384; fax: 805-893-8062; email: craig.nicholson@ucsb.edu

01 March 2016 - 31 July 2017

Research supported by the U.S. Geological Survey (USGS), Department of the Interior, under USGS Award No. **G14AP00100**. The views and conclusions contained in this document are those of the authors, and should not be interpreted as necessarily representing the official policies, either expressed or implied, of the U.S. Government.

An Integrated Onshore-Offshore Re-Evaluation of 3D Fault and Fold Geometry, Coastal Uplift and Seismic Hazard in the Santa Barbara-Ventura Area

Abstract

Based on Recent ~8-11-m uplift events of coastal marine terraces at Pitas Point, many believe these represent earthquakes near M8 on the N-dipping Pitas Point-Ventura fault (PPVF), part of the larger primarily offshore North Channel-Pitas Point-Red Mountain fault system. However, this model of multiple Holocene M8 events on the PPVF has major problems, not the least of which are: failure of the 2D fold model used to properly infer subsurface oblique 3D fault and fold geometry, an implied Holocene slip rate for the blind PPVF that is inconsistent with geologic observations or geodetic strain models, and the marked lack of near-surface fault rupture or widespread tsunami deposits expected from such shallow (<15 km depth) ~M8 events that would extend 10's of km offshore. The reason for these discrepancies may be that uplift at Pitas Point is driven primarily by slip on the S-dipping listric Padre Juan fault (PJF), by a localized restraining bend in the PPVF, or both. The PJF juxtaposes the strongly N-verging San Miguelito anticline in its hanging wall above the more symmetric Ventura Avenue-Rincon anticline in its footwall. Fault and fold geometry is well determined by industry wells that produce from the distinctly different upper San Miguelito and lower Rincon oilfields, and by imaging offshore with seismic reflection data. In the upper 3 km, the PJF exhibits up to 2.6 km of dip separation, in contrast to only ~200 m of inferred dip separation on the Ventura fault at similar depths. Much of this PJF slip is syntectonic with growth of the lower Rincon anticline as PJF splays are folded by this lower fold. The timing and slip involved for San Miguelito fold growth and its emplacement against and deformation of the lower Rincon anticline, and the geometry of the PJF and PPVF requires that much of this slip occurred while the PJF acted independently. The PJF soles into the weak Rincon Shale at a depth of ~7 km and may thus represent a classic out-of-syncline thrust. Such faults are known to generate anomalously large slip for their size and may help explain the anomalous uplift at Pitas Point. In addition, at Pitas Point, the onshore Ventura fault steps over 2 km north to the offshore Pitas Point fault. This localized restraining bend in the left-oblique-reverse PPVF may also help explain why the uplift at Pitas Point is anomalous, and not necessarily indicative of the expected slip at depth either along strike of the PPVF, or the average slip during large earthquakes. Rather, this uplift at Pitas Point is probably localized to where slip on the PJF predominates, where the PJF and PPVF strongly interact, where the PPVF restraining bend increases shortening, or some combination of all three. These factors may then limit the anticipated length, depth and slip distribution of future earthquake ruptures, and thus the seismic and tsunami hazard potential of the active fault(s) involved.

Basic observations that any model for the uplift at Pitas Point, the active subsurface 3D fault and fold geometry, or the earthquake hazard for the Santa Barbara-Ventura area must incorporate include: 1) Coastal uplift at Pitas Point is localized and anomalous, and not indicative of the uplift further along strike; 2) Pitas Point uplift is affected by two growing folds and thus by two active faults, the PPVF and PJF; 3) Growth of the mutually deforming upper San Miguelito and lower Ventura Avenue-Rincon anticlines is syntectonic, indicating that different faults acting independently are responsible for the observed fold growth; 4) Seismicity defines a steeply dipping Red Mountain fault and its prominent step north to the San Cayetano fault to depths of 18 km; 5) Both the Ventura and Pitas Point faults are blind, with little or no near-surface or near-seafloor fault rupture since the Last Glacial Maximum (LGM) and in most places offshore since 500 ka; 6) Monoclinal folding above the buried Ventura fault tip reaches a post-LGM maximum of ~24 m (or about 2-2.3 mm/yr), but diminishes offshore as the fault tip becomes deeper and rates of crustal shortening decrease westwards; 7) Hanging-wall sediments above and footwall sediments below the offshore Pitas Point fault exhibit folding and progressive tilting indicating continued late-Quaternary slip on both the PPVF and the lower PJF; 8) Oblique-slip PPVF exhibits a restraining bend at Pitas Point, which can help explain the observed localized uplift; 9) Offsets of the offshore PJF by the Pitas Point fault diminish eastward suggesting that once onshore the roles between these interacting faults may reverse, and the onshore N-dipping Ventura fault may now become primarily a secondary backthrust to the displacement-dominant S-dipping PJF.

INTRODUCTION

Accurate assessment of the earthquake hazards in southern California requires accurate and complete 3D fault maps. Many aspects of seismic hazard evaluation, including developing credible earthquake rupture scenarios, predicting strong ground motion, modeling geodetic and geologic fault slip rates, or the mechanical behavior of faults are all strongly dependent on accurately resolving the 3D geometry of active faults at seismogenic depths [*Dunham et al.,* 2011; *Herbert and Cooke*, 2012; *Lozos and Oglesby,* 2012; *Lozos et al.,* 2013, 2015; *Oglesby et al.*, 2014; *Trugman and Dunham,* 2014; *Marshall et al.,* 2013, 2014; *Shi and Day,* 2014, 2015]. Having accurate and realistic 3D models of subsurface fault geometry is also particularly important when investigating the likelihood of multi-fault ruptures in southern California, or resolving the influence of fault complexity on the distribution of surface uplift, dynamic rupture, or fold development. Because of this, the Southern California Earthquake Center (SCEC) and the US Geological Survey have consistently targeted the testing and development of new, updated and improved 3D fault models for southern California as a primary research objective. *The purpose of this project is to provide just such testing and evaluation of current fault models for the Santa Barbara-Ventura area, and the development of new, more detailed 3D fault representations for input into the SCEC Community Fault Model (CFM), based on a more extensive integrated onshore-offshore dataset and alternative interpretations for active fault and fold geometry.*

Recently, several investigators have proposed that large damaging earthquakes with magnitudes of M7.7 to M8.1 may have occurred in the western Transverse Ranges based on repeated Holocene uplift of coastal marine terraces located around Pitas Point near Ventura (**Fig.1**)[*Rockwell,* 2011; *Rockwell et al.,* 2014, 2016]. The inferred principal location for these proposed events is believed to be the Pitas Point-Ventura fault [*Hubbard et al.,* 2014; *McAuliffe et al.,* 2015; *Rockwell et al.,* 2016], part of the larger primarily offshore, N-dipping North Channel-Pitas Point-Red Mountain fault system [*Archuleta et al.,* 1997; *Kamerling et al.,* 2003; *Nicholson,* 2003, 2005; *Fisher et al.,* 2005; *Sorlien et al.,* 2014]. Owing to the increased seismic and tsunami hazard that such proposed large magnitude events would represent, and the high degree of fault complexity likely needed to generate such proposed large shallow ~M8 earthquakes, the Santa Barbara-Ventura region was designated as a Special Fault Study Area (SFSA) for focused, integrated, multi-disciplinary research [*Dolan et al.,* 2012].

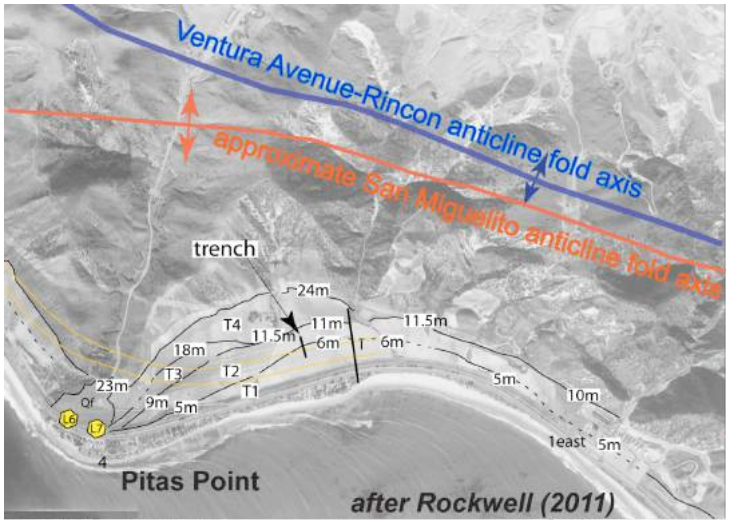

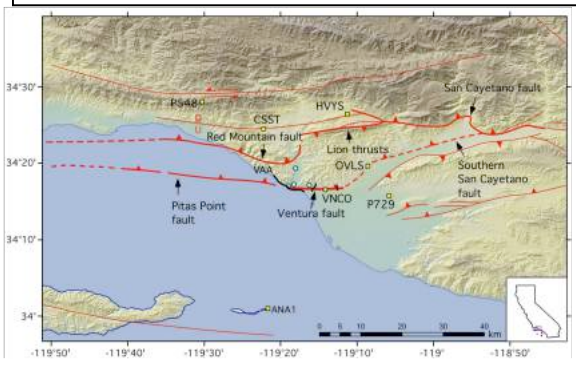

Figure 1. (left) Map of Holocene emergent terraces at Pitas Point [after *Rockwell,* 2011]. (below) Map of the eastern Santa Barbara Channel with the Pitas Point-Ventura fault.

There are, however, fundamental inconsistencies with this presumed model of multiple, large M8 Holocene events on the Pitas Point-Ventura fault, not the least of which are: the appropriateness of the 2D fault-related fold model used to infer oblique 3D fault geometry [*Nicholson and Kamerling*, 1998; *Thibert et al.,* 2005; *Nicholson et al.,* 2007], the implied Holocene slip rate for the blind Pitas Point-Ventura fault as compared to surface deformation and geodetic models [*Sorlien and Kamerling,* 2000; *Marshall et al.,* 2013, 2014], and the lack of surface rupture, seafloor offset or widespread tsunami deposits from such expected, shallow M8 events that extend offshore [*Johnson et al.,* 2013; *Reynolds et*

al., 2015]. A viable alternative interpretation, however, is that coastal uplift at Pitas Point is being driven instead primarily by slip on the S-dipping, listric Padre Juan fault (**Fig.2**)[*Grigsby,* 1988].

The emergent marine terraces at Pitas Point (**Fig.1**) are inferred to be the result of multiple 8-11 m coastal uplift events, with the latest Holocene events dated at about 0.95 ka, 2.1 ka, 4.4 ka and 6.7 ka [*Rockwell et al.,* 2016]. This uplift is inferred to occur on the south forelimb of the Ventura Avenue anticline as the direct result of slip on the Pitas Point-Ventura fault [*Hubbard et al.,* 2014; *Rockwell et al.,* 2014; *McAuliffe et al.,* 2015]. Coastal uplift at Pitas Point is, however, located directly above the backlimb of the San Miguelito anticline that is being folded above the S-dipping Padre Juan fault (**Fig.2**)[*Grigsby,* 1988; *Yeats et al.,* 1988; *Hopps et al,* 1992]. **Figure 2** shows a correlation cross section through various industry wells in the San Miguelito and Rincon oilfields below Pitas Point showing the geometry of the listric S-dipping Padre Juan fault, its near-surface upper Javon Canyon fault splay, its hanging-wall asymmetric, N-verging San Miguelito anticline, and the deeper symmetric Ventura Avenue-Rincon anticline located in its footwall. The Padre Juan fault exhibits 2.6 km of stratigraphic dip separation, and has uplifted and folded the San Miguelito anticline by nearly 2 km [*Grigsby,* 1988]. Given the age of youngest folded (not on-lapping) sediments, most of this fault slip likely occurred in the last 250,000 years or so, suggesting a shortening rate of 7-8 mm/yr for the Padre Juan fault [*Lajoie et al.,* 1982; *Grigsby,* 1988]. If on-going, this late-Quaternary rate is sufficient to account for the observed local Holocene uplift rate at Pitas Point of 6-7 mm/yr [*Rockwell et al.,* 2014; 2016] regardless of what other fault or fault-related fold processes may be also contributing to this coastal uplift.

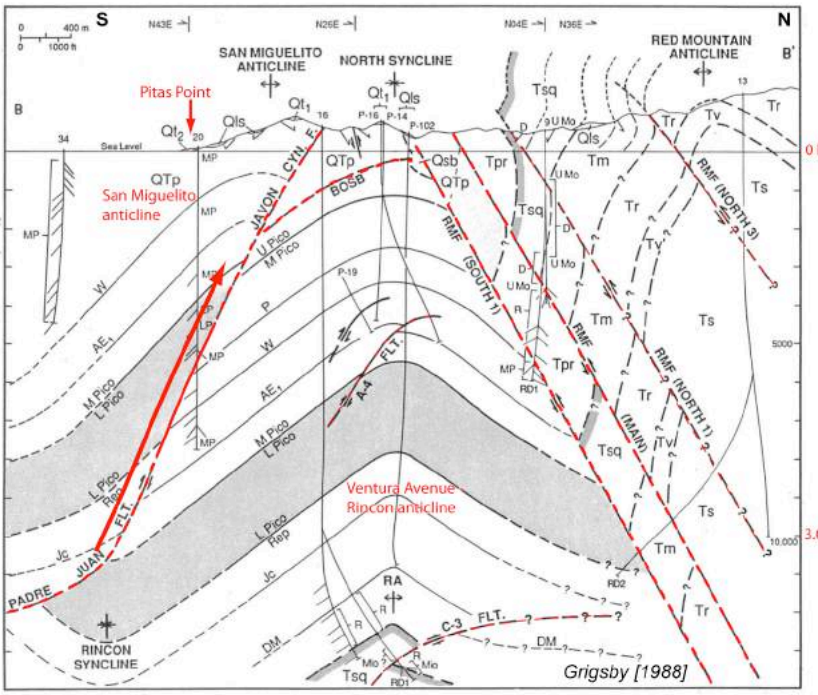

Figure 2. Correlation structure cross section looking west about 1 km west of Pitas Point of subsurface structure sampled by industry wells [*Grigsby,* 1988]. Note the S-dipping listric Padre Juan-Javon Canyon fault that thrusts the asymmetric N-verging upper San Miguelito anticline above the lower, more symmetric Ventura Avenue-Rincon anticline located in its footwall. Dip separation of top-Lower Pico Formation (shaded) along Padre Juan fault is 2.6 km (red arrow). Most of this fault slip is post-250 ka [*Grigsby,* 1988], coincident with Ventura Avenue fold growth. Pitas Point is located directly above the active Padre Juan fault. Uplift at Pitas Point is therefore likely the result of slip on—and folding above—the out-of-syncline Padre Juan fault, in addition to potential uplift of the lower Ventura Avenue-Rincon anticline. Faults on right are various strands of the N-dipping Red Mountain fault.

In addition to S-dipping structures like the Padre Juan fault, different fault models and alternative representations have also been proposed for the N-dipping North Channel-Pitas Point-Red Mountain fault system. **Figure 3** shows revised alternative fault sets for this N-dipping fault system available in the SCEC CFM-v5.0 as of the start of this project [*Plesch et al.,* 2014; *Nicholson et al.,* 2014]. The set on the left is from the Harvard group and is based mostly on a 2D fault-related fold model and a limited set of well data in the onshore Ventura basin [*Hubbard et al,* 2014]. The set on the right is largely from UCSB and is based on mapping 3D fault surfaces with industry seismic reflection and well data (**Fig.4**), and combining this with relocated seismicity in the offshore Santa Barbara Channel [*Kamerling et al.,* 1998, 2003; *Nicholson and Kamerling,* 1998; *Nicholson et al.,* 2014]. The major difference between these alternative interpretations is the degree to which N-dipping oblique faults, like the Pitas Point-Ventura and Red Mountain faults that merge at depth, are offset (or not) by a near-flat detachment at a depth of about 7 km. Geologic evidence for such potential detachments or bedding-plane slip surfaces, is

provided by the presence of the mechanically weak Rincon Shale and other shale layers in younger strata, however, these weak shale layers and detachments typically dip south, not north, in and around the Santa Barbara-Ventura area [*Yeats et al.,* 1988]. As a result, these mechanically weak layers have facilitated gravity sliding mainly southwards towards the basin from surrounding northern uplifted regions, and subsequent development of non-planar 3D fault geometry [*Nicholson et al.,* 2007].

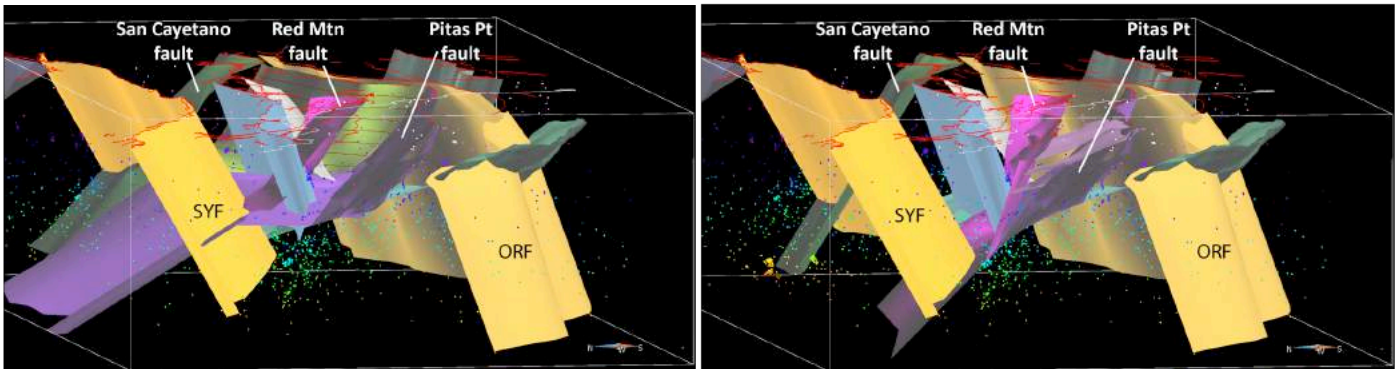

Figure 3. Oblique 3D views looking East of active faults in the Ventura-Santa Barbara area relative to relocated seismicity (dots) [*Plesch et al.,* 2014]. (*left*) CFM-v5 models with midcrustal detachment from *Hubbard et al* [2014] for Pitas Point, Ventura, Red Mountain, Lion, San Cayetano, and South San Cayetano faults. (*right*) Updated CFM-v5 models without mid-crustal detachment and slightly steeper dips for the Pitas Point, North Channel, Red Mountain, Arroya Parida-Mission Ridge, San Cayetano and Santa Ynez faults [*Kamerling et al*., 2003; *Nicholson et al.,* 2014].

These models and their alternative representations need to be tested and evaluated to see which fault set, or combination of intersecting and potentially interacting faults, best fits the observations and patterns of surface deformation. These fault models also need to be further updated and improved, as several faults are somewhat incomplete. For example, the CFM-v5.0 models for the Pitas Point-Ventura, North Channel and Red Mountain faults only extend west to Coal Oil Point near UCSB. Subsequent mapping with multichannel seismic (MCS) reflection data documents that these active fault structures extend from Ventura past Pt. Conception, a distance of over 120 km (**Fig.4**)[*Sorlien et al.,* 2014]. The CFM-v5.0 fault models can also be updated and expanded to incorporate additional alternative interpretations and important fault and fold details not currently accounted for in existing CFM fault sets. This specifically includes the presence of active S-dipping thrust faults, like the Padre Juan fault (**Fig.2**), that have also contributed to near-surface folding and coastal uplift.

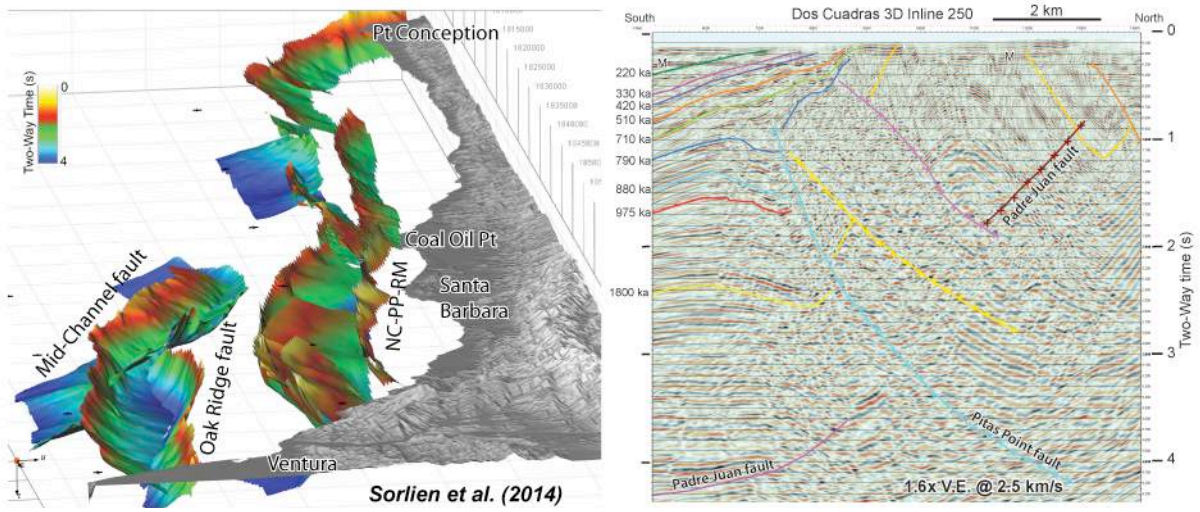

Figure 4. (left) Oblique view looking west of N-dipping North Channel-Pitas Point-Red Mountain fault system extending from Ventura to Pt. Conception based on mapping with industry MCS data [*Sorlien et al.,* 2014]. (right) Example of in-line slice from 3D seismic survey used to help map the blind, non-planar Pitas Point fault (blue) and dated seismic stratigraphy (colored horizons) that document rates of deformation, uplift and fold development [*Sorlien et al.,* 2014].

The purpose of this project is to test and evaluate existing CFM fault models and to develop new alternative 3D fault representations for the Santa Barbara-Ventura area, including their related fold geometry and expected patterns of coastal uplift and fault slip. High-resolution marine seismic reflection data will be used to estimate rates of Recent offshore fault slip and fold development, and compared with the fault slip predicted from observed coastal uplift and related dynamic rupture models [*e.g., Rockwell et al.,* 2016; *Ryan et al.,* 2015]. Deeper onshore and offshore 3D fault geometry, including alternative fault representations (*e.g.,* **Fig.3**) will be evaluated using relocated earthquake hypocenters [*Hauksson et al.,* 2012 + updates] and focal mechanisms, grids of deep-penetration industry MCS data (**Fig.4**)[*Sorlien and Nicholson*, 2015], and a more extensive set of onshore-offshore well data [*Hopps et al.,* 1992; *Redin et al.,* 2005]. New alternative interpretations of the complex fault and fold geometry that include previously mapped S-dipping thrust faults, like the Padre Juan fault (**Fig.2**), and updated 3D fault maps of the offshore North Channel-Pitas Point fault system (**Fig.4**) that extend this system farther west will also be incorporated into revised 3D fault models for CFM. These alternative fault models may then explain why the observed coastal uplift at Pitas Point should be considered anomalous, and not representative of either adjacent fault slip, or the average fault slip expected at depth during dynamic earthquake rupture. The primary products of this project will then be: 1) an improved understanding of the active fault and fold structures driving the pattern of observed coastal uplift and related coastal hazards, and 2) a set of improved, updated 3D fault representations for the revised SCEC CFM as reflected in CFM version 5.1 [*Plesch et al.,* 2016] and version 5.2 [*Nicholson et al.,* 2017].

DATA AND METHODS

To evaluate the existing CFM 3D fault set, to update and expand CFM with new 3D fault models, and to help discriminate between proposed alternative fault representations, a fully integrated, multi-disciplinary onshore-offshore dataset was developed for the Santa Barbara-Ventura area. This dataset includes among other things: high-resolution and deep-penetration marine MCS reflection data, onshore/offshore industry well data, industry correlation structure contour maps and cross sections, relocated seismicity and revised focal mechanism catalogs, digital onshore topography and offshore bathymetry data, and onshore/offshore geologic maps. In addition, a set of well-dated stratigraphic reference horizons [*Yeats,* 1981; *Sorlien and Kamerling,* 1998; *Nicholson et al.,* 2006, 2007; *Marshall et al.,* 2012; *Johnson et al.,* 2013; *Sorlien and Nicholson,* 2015; *Behl et al.,* 2016] have been identified and mapped that, combined with geodetic and GPS strain models [*Sylvester,* 2000; *Marshall et al.,* 2013], provide estimates of cumulative finite deformation, rotation, fault offset and fold development, as well as modern, Recent, Quaternary, and older rates of uplift, subsidence, shortening and fault slip [*e.g., Gratier et al.,* 1999; *Sorlien and Kamerling,* 2000; *Sorlien et al.,* 2000; *Thibert et al.,* 2005; *Nicholson et al.,* 2007; *Marshall et al.,* 2013; *Sorlien and Nicholson,* 2015; *Johnson et al.,* 2017].

High-resolution and Deep-penetration Marine Multi-Channel Seismic (MCS) Reflection Data

As part of a long history of industry hydrocarbon exploration and field development, and mapping of potential coastal and seafloor hazards, extensive grids of high-resolution and deep-penetration MCS reflection lines were acquired in the Santa Barbara Channel. This included both 2D and 3D seismic reflection surveys. **Figure 5** shows only part of a basemap of these data that were used to correlate and map offshore 3D fault and fold structure and dated stratigraphic reference horizons (**Fig.4**) [*Sorlien et al,* 2014, 2015; *Sorlien and Nicholson*, 2015]. A vertical time slice (Inline 250) from the Dos Cuadras 3D seismic survey that images the Pitas Point and Padre Juan faults is shown in **Figure 4** (*right*). This figure shows a number of the dated (colored) stratigraphic reference horizons that could be mapped in 3D to document the timing and rate of fault and fold development. This figure documents that in this area east of Santa Barbara: 1) the S-dipping Padre Juan fault is imaged in the hanging wall and footwall of the N-dipping Pitas Point fault; 2) the Padre Juan is offset by the Pitas Point fault; 3) the Pitas Point fault is blind and does not offset sediments younger than about 500 ka; 4) progressive fold limb rotation above the Pitas Point fault indicates that continued fault slip decreases updip and is absorb by hanging-wall folding; and 5) minor folding south of the Pitas Point fault (in its footwall) indicates continued Quaternary slip on the lower Padre Juan fault [*Sorlien et al.,* 2014, 2016; *Nicholson et al.,* 2015, 2016].

Figure 5. Part of the basemap of 2D MCS lines and 3D seismic surveys (green grids) used to correlate and map offshore faults, folds and stratigraphic reference horizons in 3D (*e.g.,* **Fig.4**)[*Sorlien et al.,* 2014; *Sorlien and Nicholson,* 2015]. Also shown are tip lines or surface traces of mapped faults and the well locations used to construct the correlation cross sections near Pitas Point (*e.g.,* **Figs.2&8**)[*Grigsby,* 1988; *Hopps et al.,* 1992].

Compare the fault and fold structure imaged by Dos Cuadras Inline 250 (**Fig.4,** *right*) with that imaged by a similar industry two-way travel-time (twtt) section located farther east closer to Pitas Point (**Fig.6**). In this MCS time section, both the S-dipping listric Padre Juan and N-dipping Pitas Point faults are again well imaged. Both faults contribute to the uplift and folding of the asymmetrical N-verging hanging-wall fold that is the offshore equivalent of the onshore N-verging San Miguelito anticline found above the Padre Juan fault at Pitas Point (**Fig.2**). Additional footwall folding below (and south of) the Pitas Point fault is again likely related to continued slip on the lower Padre Juan fault. At this location, the Pitas Point fault is still completely blind, and exhibits no fault rupture of shallow sediments since ~500 ka. The difference is that the apparent vertical separation of the upper and lower Padre Juan fault by the Pitas Point fault has significantly decreased to the point that it is difficult to tell if either fault actually offsets the other. This suggests—but does not prove—that once onshore, the roles between the Padre Juan and Pitas Point faults may flip, and the Padre Juan fault may become the dominant displacement fault.

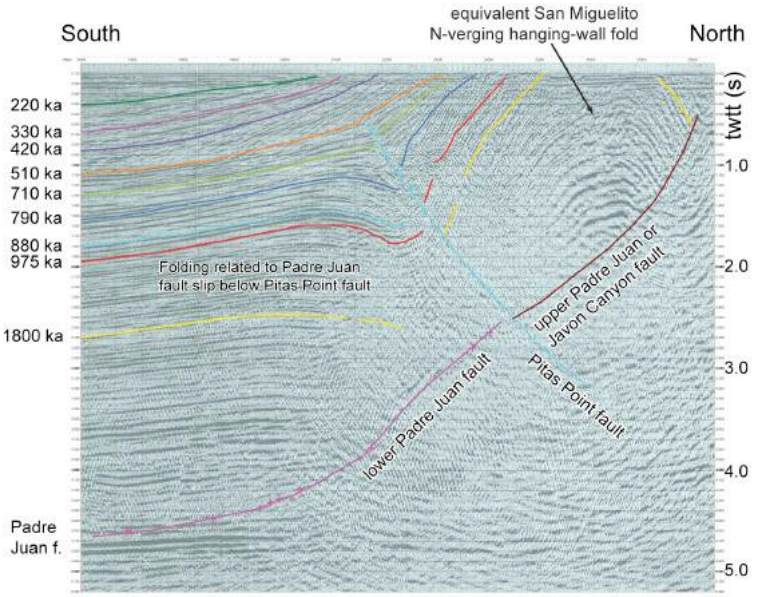

Figure 6. Industry MCS reflection line located ~10 km west of Pitas Point (**Fig.5**). Both the N-dipping, blind Pitas Point (blue) and S-dipping, listric Padre Juan (purple) faults are well imaged. Both contribute to the N-verging asymmetrical hanging-wall fold equivalent to the onshore San Miguelito anticline. However, here the upper and lower Padre Juan faults show little apparent vertical separation across the Pitas Point fault, suggesting that either could become the dominant offsetting, displacement fault farther east onshore [*Nicholson et al.,* 2015, 2016].

In addition to the deep-penetration MCS data that are capable of imaging stratigraphy, faults, and fault-related fold structures to depths of 6-7 km, grids of high-resolution seismic reflection data were also acquired as part of various seafloor hazard and coastal hazard mapping programs [*Richmond et al.,* 1981; *Burdick and Richmond,* 1982; *Sliter et al.,* 2008; *Johnson et al.,* 2013]. **Figure 7** shows one of the high-resolution marine USGS minisparker lines (SB-78) that cross the Pitas Point fault [*Johnson et al.,* 2016]. Holocene (H) sediments since the Last Glacial Maximum (LGM) lowstand are shaded in yellow. The angular LGM unconformity—which in this area is estimated to be ~10-12 ka [*Reynolds and Simms,* 2015]—is easily identified and mapped with these data [*Johnson et al.,* 2013, 2017], and thus provides a well-dated reference horizon that documents cumulative finite strain, fault offset or fault-related folding since it formed. This seismic line indicates that since the LGM unconformity, ~12 m of monoclinal folding occurred above the blind Pitas Point fault—the fault itself exhibits no near-seafloor or Holocene fault rupture. The data also document progressive tilting and limb rotation both above (north of) and below (south of) the fault that likely indicates continued Quaternary slip on both the Pitas Point fault, and the Padre Juan fault located in its footwall [e.g., *Sorlien et al.,* 2015, 2016; *Nicholson et al.,* 2016].

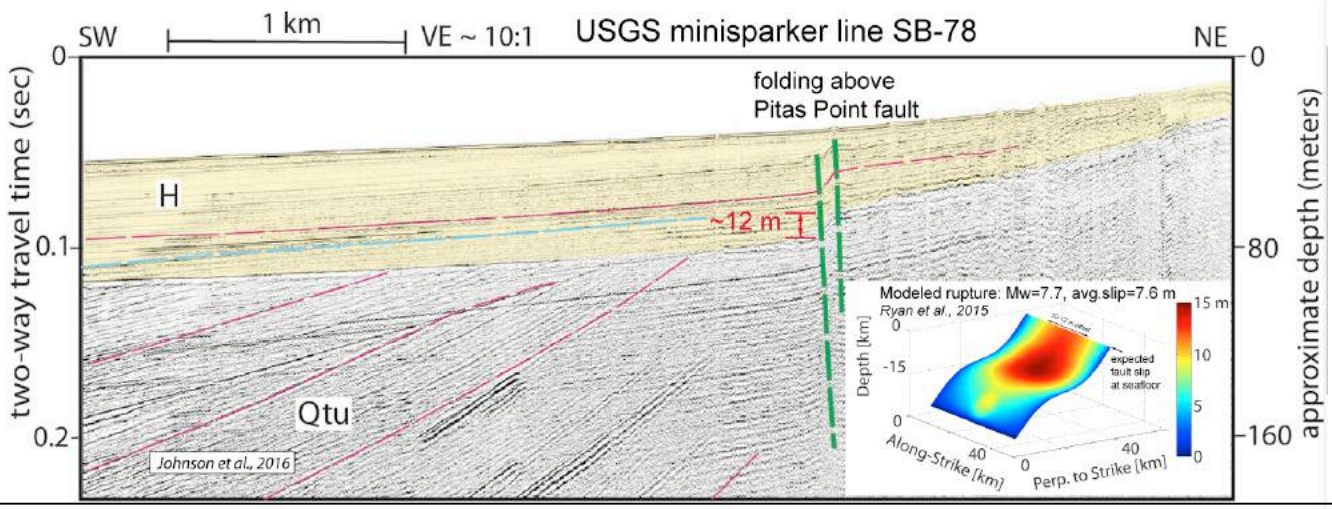

Figure 7. High-resolution USGS minisparker line SB-78 across the blind Pitas Point fault just south of Pitas Point [*Johnson et al.,* 2016]. Sediments deposited since the Last Glacial Maximum (LGM) are shaded yellow. Note progressive tilting above and below the Pitas Point fault. Green lines are fold axes, not fault surfaces. (*inset*) Dynamic rupture model of the Pitas Point fault with moment magnitude M7.7, average slip=7.6 m, and predicted seafloor fault offset of ~10-12 m [*Ryan et al.,* 2015]. Based on this model, expected seafloor offset from multiple uplift events at Pitas Point would exceed 50 m, yet in most places, post-LGM sediments show no such fault offset.

Onshore-Offshore Industry Well Data

Besides the subsurface imaging and structural interpretation capability afforded by the MCS data, there is also the important structural and stratigraphic information provided by industry well data. A distinct advantage to working in this area is the wider availability of onshore and offshore industry seismic and well data with which to image and ground truth subsurface 3D fault and fold geometry, and to map deformed stratigraphic reference horizons (**Figs.2,4-6**) [c.f., *Yeats,* 1981; *Grigsby,* 1988; *Yeats et al.,* 1988; *Hopps et al.,* 1992; *Sorlien and Kamerling,* 2000; *Kamerling et al.,* 2003; *Redin et al.,* 2005; *Thibert et al.,* 2005; *Nicholson et al.,* 2007; *Sorlien et al.,* 2014, 2015; *Sorlien and Nicholson,* 2015]. These datasets have been used to construct numerous structure maps and correlation cross sections that can help guide 3D fault-and-fold interpretations. For example, *Hopps et al.* [1992] used nearly 1200 deep-penetrating wells to develop 17 structure contour maps and 84 interlocking cross section data panels for the onshore Ventura basin (https://projects.eri.ucsb.edu/hopps/). *Redin et al.* [2005] used another ~250 wells to construct 11 correlation cross sections across the Santa Barbara Channel and nearshore Ventura basin (*e.g.,* **Fig.8**). In contrast, *Hubbard et al.* [2014] used 15 selected wells up to 16 km off-axis to define one, single 2D fault-related fold model. For this project, these valuable industry well data were incorporated into its updated integrated subsurface dataset [*Nicholson et al.,* 2015, 2016].

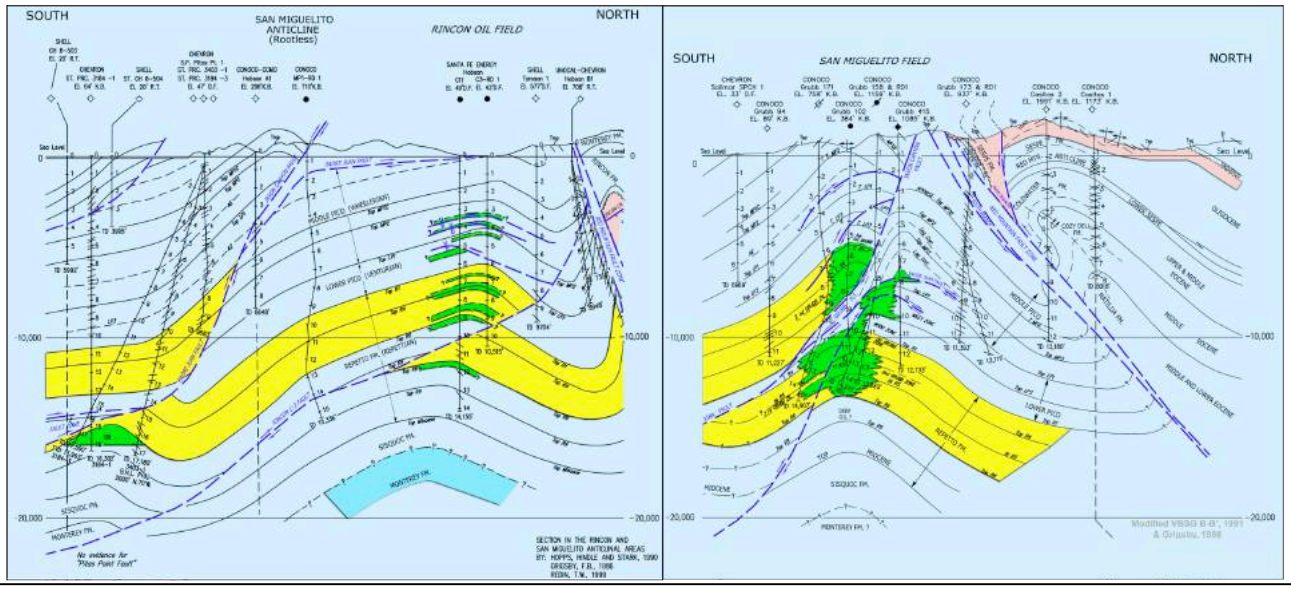

Figure 8. Correlation cross sections from industry wells along lines located about 1 km west (*left*) and 3 km east (*right*) of Pitas Point [*Redin et al.,* 2005]. The dominant structure drilled by wells directly below Pitas Point is the N-verging San Miguelito anticline and S-dipping Padre Juan-Javon Canyon fault. Continuity of strata and absence of fault cuts in wells south of Pitas Point limit the dip, location and 3D geometry of the Pitas Point-Ventura fault.

Relocated Seismicity Catalogs

A critical resource in terms of evaluating mapped 3D faults, discriminating between alternative fault representations in CFM, or extending 3D fault surfaces defined by MCS and well data to seismogenic depths is the extensive set of relocated earthquake hypocenter and focal mechanism catalogs [*Hauksson et al.,* 2012, 2016; *Yang et al.,* 2012], and other independent catalogs of relocated aftershocks and regional seismicity [*Bogaert,* 1984; *O'Connell,* 1995; *Nicholson and Kamerling,* 1998]. These relocated seismicity catalogs often represent the only available data to accurately define active fault surfaces at seismogenic depths. When evaluated in combination with kinematic analysis of earthquake focal mechanisms, these datasets can resolve the sense of fault slip and non-planar 3D fault surfaces at depth [*Nicholson and Kamerling*, 1998; *Nicholson et al.,* 2012, 2015]. A simple example is demonstrated by alignment of hypocenters downdip of the Pitas Point, Red Mountain, Arroyo Parida and Santa Ynez faults, and the curviplanar alignment of hypocenters and nodal planes to define an older, ancestral Santa Ynez fault (ASYF)(**Fig.9**, *left*)[*Nicholson,* 2013]. Recent seismicity is often found clustered at the intersection of the Red Mountain and Pitas Point faults, with a few events on the lower Padre Juan fault (**Fig.9**, *right*) indicating that both the Pitas Point and lower Padre Juan faults are seismically active.

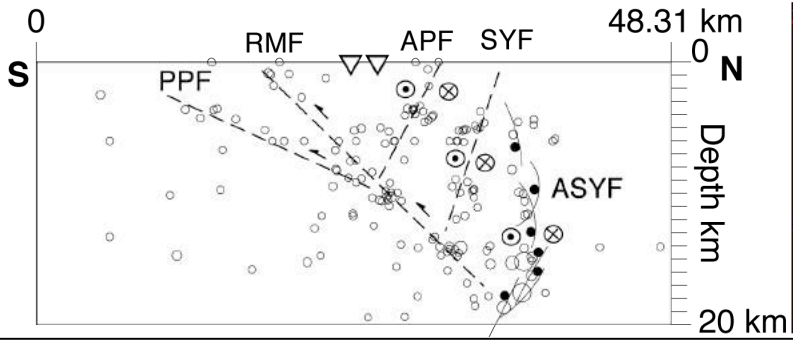

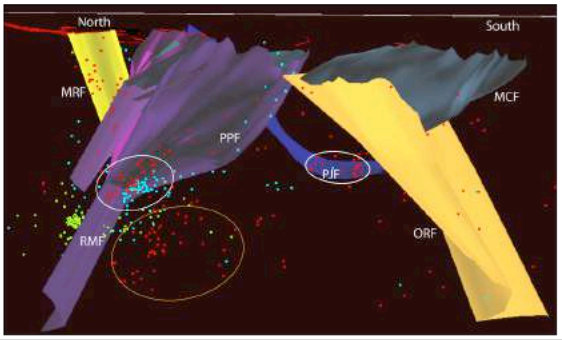

Figure 9. (*right*) Cross section of relocated seismicity across eastern Santa Barbara Channel that define Pitas Point (PPF), Red Mountain (RMF), Arroyo Parida (APF), Santa Ynez (SYF) and ancestral Santa Ynez (ASYF) faults [*Nicholson and Kamerling*, 1998]. Note systematic change in nodal plane dip with depth to define a curviplanar, primarily strike-slip ASYF associated with the 1996 M4.6 Ojai sequence. (*left*) Oblique 3D view of recent relocated hypocenters and CFM-v5.1 faults. Events are clustered on the lower Padre Juan fault (PJF) and near the intersection of the RMF and PPF (white circles). Earthquakes are also found at greater depth below the PPF (orange circle) related to additional footwall deformation.

RESULTS AND DISCUSSION

Proper Identification and Characterization of Fault-Related Fold Interaction

A primary source of confusion is the misidentification of the separate and distinct N-verging San Miguelito anticline as the deeper, more symmetrical Ventura Avenue anticline (**Fig.10**)[*Rockwell,* 2011; *Pacific Section-AAPG,* 2014]. This leads to the false assumption and mischaracterization that there is only one active fault-related fold that drives coastal uplift near Pitas Point and Ventura, i.e., the Ventura Avenue-Rincon anticline [*Hubbard et al.,* 2014; *McAuliffe et al.,* 2015; *Rockwell et al.,* 2016]. However, industry well data (**Figs.2&8**) and imaging with MCS data (**Fig.6**) clearly document a separate N-verging San Miguelito fold above a listric S-dipping Padre Juan fault that *actively deforms and is itself deformed by* a lower Ventura Avenue-Rincon anticline [*Grigsby,* 1988; *Yeats et al.,* 1988; *Hopps et al.,* 1992; *Redin et al.,* 2005; *Nicholson et al.,* 2015]. Given the relative ages of the San Miguelito anticline (<250 ka) [*Grigsby,* 1988], the Ventura Avenue anticline (<200-300 ka) [*Rockwell,* 1988], and inferred initiation (<100 ka) and emergence (<30 ka) of the N-dipping Ventura fault [*Hubbard et al.,* 2014], this necessarily requires that the fault slip required to produce the San Miguelito and Ventura Avenue folds is both syntectonic and independent. This is because fault slip needed to drive Ventura Avenue fold growth can not simultaneously drive additional uplift and folding of the N-verging San Miguelito fold.

Figure 10. This is NOT the Ventura Avenue anticline! It is the distinctly separate San Miguelito anticline! This classic amphitheatre photo looking west is often mistaken for the Ventura Avenue anticline [*e.g., Rockwell,* 2011], which is located below and farther east along trend. However, this is the asymmetrical N-verging San Miguelito anticline and oilfield. Pitas Point is located at the coast just off the photo at left. Photo credit Art Sylvester.

Many cross sections near Pitas Point do not show the Ventura or Pitas Point fault (**Figs.2&8**) owing mainly to a lack of near-surface offset [*Grigsby,* 1988; *Hopps et al.,* 1992; *Redin et al.,* 2005]. If the cross section near Pitas Point is updated to include the Ventura fault (**Fig.11**), given its mapped location and geometry from its near-surface trace and subsurface data [*e.g., Sarna-Wojcicki et al,* 1976; *Sarna-Wojcicki and Yerkes,* 1982; *Hubbard et al.,* 2014] then the relative contributions of the S-dipping Padre Juan and N-dipping Ventura faults to the uplift and fold growth at Pitas Point can be more easily understood. As previously noted, the listric Padre Juan fault juxtaposes the strongly N-verging San Miguelito anticline in its hanging wall above the more symmetric Ventura Avenue-Rincon anticline in its footwall. Fault and fold geometry is well determined by industry wells that produce from the distinctly different upper San Miguelito and lower Rincon oilfields (**Figs.2,8&11**), and by imaging offshore with seismic reflection data (**Fig.6**). In the upper 3 km, the Padre Juan exhibits up to 2.6 km of dip separation, in contrast to ~200 m of inferred dip separation on the Ventura fault at similar depths (**Fig.11**). Much of this Padre Juan slip is syntectonic with growth of the Rincon anticline as Padre Juan splays are folded by this lower fold. The timing and slip involved for San Miguelito fold growth and its emplacement against and deformation of the lower Rincon anticline, the specifics of inferred Ventura fault propagation, and the active fault geometry requires that much of this fault slip occurred while the Padre Juan fault acted independently, and not as a supposed backthrust to the Pitas Point-Ventura fault [*Nicholson et al.,* 2016]. This is because a fault can not by itself transfer material or slip from its

footwall to its hanging-wall block; nor can a fault (Ventura fault) drive uplift of its principal hanging-wall fold (Ventura Avenue anticline) while syntectonically driving the uplift and folding (San Miguelito anticline) on a presumed backthrust. Retrodeforming Padre Juan fault slip and San Miguelito fold growth requires that this fold material move back from the hanging wall to the footwall of the Ventura fault. This indicates that the Ventura fault did not contribute to the emplacement of this fold. In addition, projecting the location and dip of the Ventura fault below the Padre Juan (dashed blue line, **Fig.11**) suggests that the Ventura fault above the Padre Juan has been displaced north relative to its presumed position below the fault south of the Ventura Avenue fold axis.

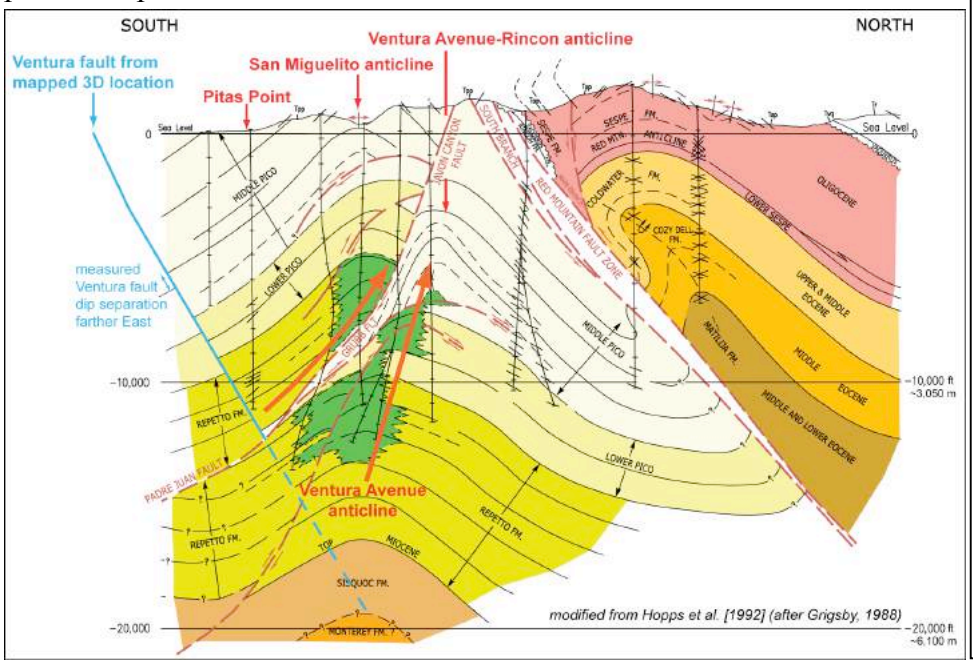

Figure 11. Revised cross section 3 km west of Pitas Point from industry well data [*Nicholson et al.,* 2016]. Note Padre Juan fault slip is syntectonic with growth of lower Rincon anticline as San Miguelito anticline emplacement both deforms this lower fold and Padre Juan fault splays are also folded. Padre Juan fault slip is independent of Ventura fault slip because upper fold emplacement requires moving material from the footwall to the hanging wall of the Ventura fault. Above 3 km, Ventura fault dip separation is ~200 m. Given fault dip and depth below Pitas Point, an 8-m uplift event would correspond to >10-m of fault slip at depth.

To emphasize this last point and the fundamental inconsistencies of the published 2D fault-related fold model for the Ventura fault and Ventura Avenue anticline [*Hubbard et al.,* 2014], both the 2D model and the actual subsurface fault and fold structure below Pitas Point (**Fig.11**) are shown at the same scale and aligned with the older, initial lower fold axis of the Ventura Avenue anticline (**Fig.12**). This figure documents that: 1) the 2D model does not have the correct location and dip of the Ventura fault relative to its principal Ventura Avenue fold axis; 2) it does not account for the presence of the S-dipping Padre Juan fault, the syntectonic N-verging San Miguelito anticline, or the deformation of the lower Ventura Avenue anticline by this upper fold; 3) it does not account for the presence or correct dip of the Red Mountain fault strands or its fairly rigid—as compared with basin sediments—hanging-wall block. Because of this, previous interpretations model growth of the more symmetrical Ventura Avenue anticline as primarily the result of S-dipping faults buttressed against the more rigid Red Mountain fault.

To be valid, the 2D model needs to account not only for the observed complex 3D fault and fold structure, it also needs to substantiate the assumptions used in its model construction. These include: 1) structure is fundamentally 2D, which allows the projection of well and dipmeter data by up to 16 km; 2) the footwall is rigid and non-deforming, and defined by a ramp-flat-ramp fault geometry with faults that dip at less than 45°; and 3) all deformation is in the plane of the cross section, which precludes strike-slip or oblique-slip on faults. However, none of these model assumptions are correct [*Nicholson and Kamerling,* 1998]. Structure is not 2D, it's 3D [*Yeats et al.,* 1988; *Hopps et al.,* 1992; *Nicholson et al.,* 2007, 2015] and dipmeter data should not be projected more than 100 m, much less than over 10 km. The footwall is not rigid, but rapidly deforming and subsiding [*Yeats,* 1981; *Nicholson et al.,* 2007]. This precludes the existence and preservation of a flat, rigid, horizontal detachment in the basin that is a key component of the 2D model, and without which the model fails. Faults also typically exhibit evidence of oblique slip, or evidence for reactivation of inherited strike-slip or oblique-normal faults. This results in most faults exhibiting dips of 50° or more, not the lower dips assumed for the 2D model.

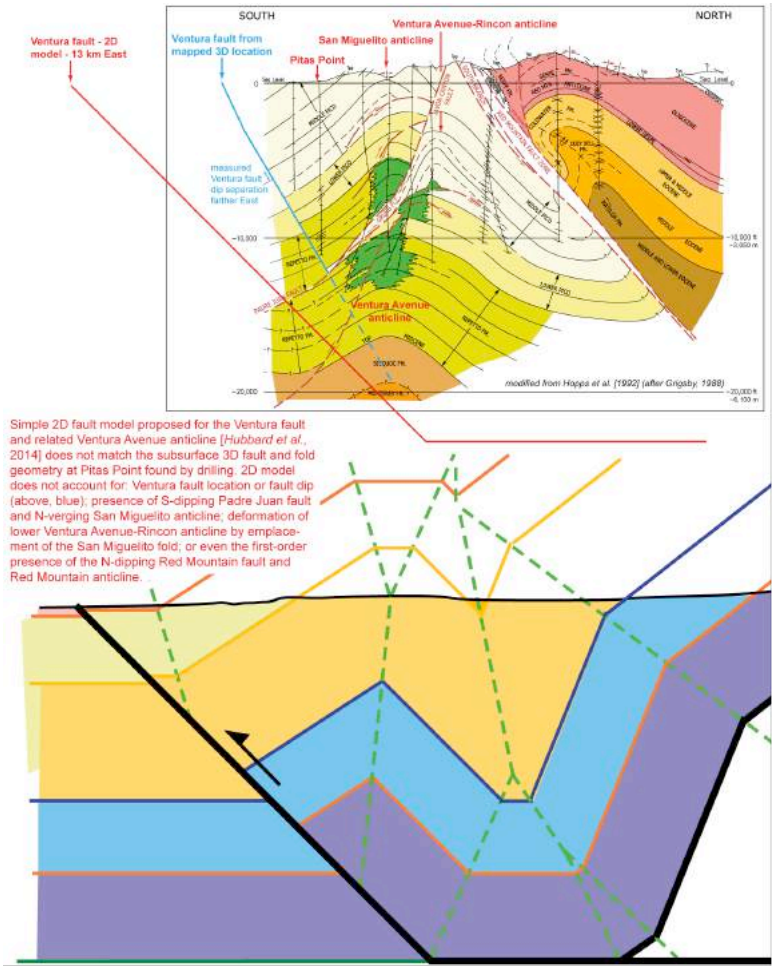

Figure 12. (*top*) Subsurface fault and fold structure drilled by industry wells near Pitas Point. (*bottom*) 2D fault-related fold model for the emergent N-dipping Ventura fault and related Ventura Avenue anticline [*Hubbard et al.,* 2014]. Both figures are to the same scale and aligned along the initial, deep Ventura Avenue fold axis.

The question remains, however, as to whether currently, the blind Ventura fault is acting as a backthrust to the Padre Juan fault or *vice versa*. Arguments in favor of the onshore Ventura fault (not the offshore Pitas Point fault) acting as a backthrust include: 1) Both the Ventura and Padre Juan faults are considered Holocene active based on the same geologic criteria by the same people [*Sarna-Wojcicki et al.,* 1976, 1987], and the offshore lower Padre Juan appears to be seismically active (**Fig.9**, *right*); 2) the cumulative late-Quaternary fault offset in the upper 3 km for the Padre Juan fault is an order of magnitude higher than the younger, emergent Ventura fault (**Fig.11**), indicating that at this location onshore, it is the dominant displacement fault at this shallow structural level; 3) when last imaged just offshore (**Fig.6**), it can not be resolved which of the oppositely dipping faults (Padre Juan or Pitas Point) offsets the other, but Pitas Point fault offsets are becoming less dominant farther east; and 4) as mentioned, the Ventura fault seems to be displaced north (i.e., offset) by the Padre Juan fault relative to its expected undeformed location below the Padre Juan (red line, **Fig.12**), if it had produced the lower Ventura Avenue-Rincon anticline and should be south of the lowermost fold axis.

Arguments in favor of the Padre Juan fault acting as a backthrust to the Ventura fault and may be to some extent now inactive, once the Ventura fault is inferred to have broken through to the surface at ~30 ka [*Hubbard et al.,* 2014; *Rockwell et al.,* 2016], include: 1) the dominance of the N-dipping Pitas Point fault offshore and the clear offsets of the Padre Juan fault by the Pitas Point fault; 2) the evidence for Holocene folding, fold scarps and uplift events above the blind Ventura fault, indicating a Recent preference for Ventura fault slip at depth; and 3) the lack of evidence for similar Holocene uplift events or fault slip at the surface trace of the Javon Canyon fault [*T.Rockwell,* pers.comm., 2016]. However, it should be noted that the roles of oppositely dipping faults can switch along strike, the uplift events found at the Ventura fault [*McAuliffe et al.,* 2015] do not all match the timing or number of uplift events at Pitas Point [*Rockwell et al.,* 2016](so where did the slip for the other uplift events come from?), much of Padre Juan fault slip is absorbed by increased tight folding at depth (as shown by BOSB, 'Base of Steep Beds', **Fig.2**) and not necessarily expressed as surface fault offset along its upper Javon Canyon fault splay, and the unusually large late-Quaternary displacement of the Padre Juan fault that soles out into the Rincon Shale at ~7 km depth suggests this fault is acting as a classic out-of-syncline thrust (OOST).

A key point that many people seem to have forgotten is that the mechanically weak Rincon Shale and other shale layers in younger basin strata facilitate the occurrence of such out-of-syncline thrust faults in active compressional basins. Once active, these out-of-syncline thrusts are notorious for exhibiting anomalous displacements and high slip rates for their size, owing to the low-friction, bedding-plane surfaces they typically occupy. A triggered M2.3 OOST earthquake in a diatomite quarry near

Lompoc, CA produced anomalous surface fault offsets [*Sylvester and Heinemann*, 1996] normally associated with a magnitude M6.2 event. These weak shale layers onshore and offshore of Ventura are imaged as forming the basal thrust into which S-dipping faults, like the Sisar and Padre Juan faults typically sole [*Yeats et al.*, 1988; *Kamerling et al.,* 2003; *Sorlien et al.,* 2016]. These out-of-syncline thrust faults can more easily accommodate the volumetric strains and space problems generated by the rapid convergence across the deep, subsiding Ventura basin, one of the deepest compressional basins in the world [*Yeats et al.,* 1994; *Nicholson et al.,* 2007]. As such, out-of-syncline thrust faults like the Padre Juan fault and Sisar detachment [*Yeats et al.,* 1988] are likely to remain active as long as the basin continues to shorten, and space problems continue to develop as the major E-W fault systems like the North Channel-Pitas Point-Red Mountain and Oak Ridge fault systems continue to converge eastward.

Development of New, Updated 3D Fault Models

As part of our on-going group efforts to update, expand and improve CFM, a major component of this project was the development of new, updated 3D fault models for the Santa Barbara-Ventura area. These revised fault models incorporate new alternative interpretations of complex 3D fault-and-fold geometry (**Figs.6&11**), as well as recently updated 3D fault maps of the offshore North Channel-Pitas Point-Red Mountain and Oak Ridge fault systems (*e.g.,* **Fig.4**)[*Sorlien et al,* 2014, 2015, 2016]. For this project, offshore fault surfaces and deformed, dated stratigraphic reference horizons from a previous USGS project [*Sorlien and Nicholson,* 2015] that were mapped in two-way travel-time (twtt) with MCS data (**Fig.4**) were first depth-converted using the Harvard 3D velocity model (CVM-H), augmented with existing well data (*e.g.,* **Fig.8**), smoothed, merged and integrated with the more complex 3D fault and fold structures mapped onshore (e.g., **Fig.11**), and extended to seismogenic depths based on available relocated seismicity (**Figs.3&9**)[*Nicholson et al.,* 2016]. Recent 3D fault updates to CFM thus include: extending the active North Channel-Pitas Point-Red Mountain fault system west to Pt. Conception, updating the geometry of the offshore Oak Ridge and Mid-Channel faults, incorporating S-dipping detachment faults in the western, eastern, and mid-channel areas, including the Hondo, Padre Juan and Western Deep faults, and adding onshore faults like the Javon Canyon and Sisar detachment (**Fig.14**), based on structural interpretations and 3D mapping with our more extensive integrated onshore-offshore dataset of MCS, well and seismicity data [*Sorlien et al.,* 2016; *Nicholson et al.,* 2015, 2016].

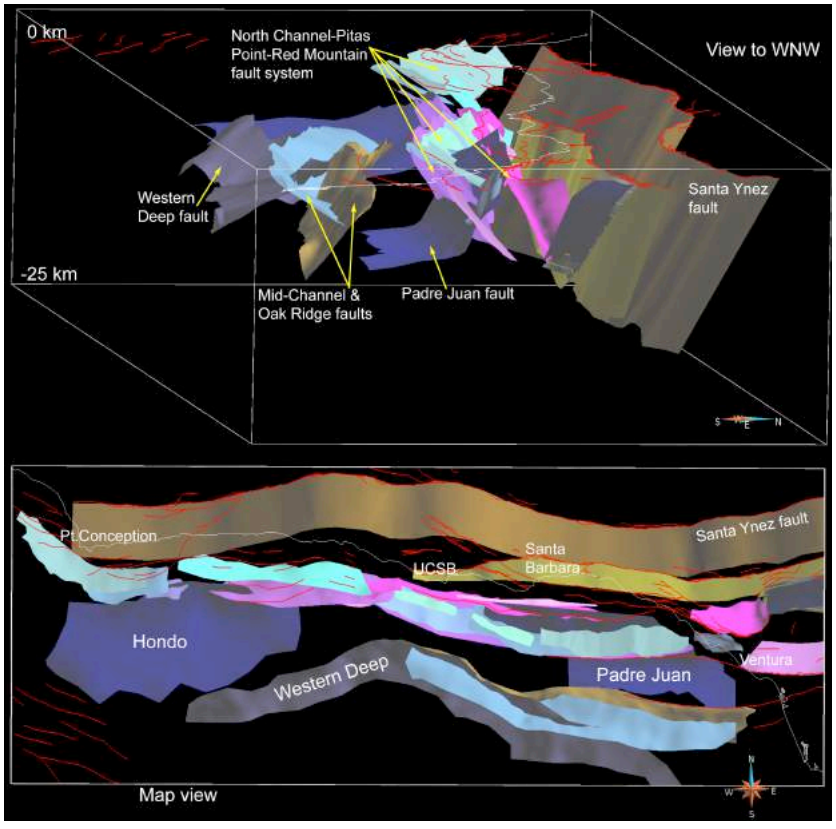

Figure 14. (*top*) Oblique 3D view looking WNW of CFM-v5.1 fault models in the Santa Barbara Channel, onshore Santa Ynez Range and western Ventura basin. (*bottom*) Map view of same CFM faults. Red lines are USGS/CGS Quaternary fault surface traces; fine white line is coast line. New or updated fault models were added to CFM for the onshore Ventura fault, North Channel-Pitas Point-Red Mountain fault system, the Oak Ridge and Mid-Channel faults, and S-dipping Hondo, Western Deep, Padre Juan, Javon Canyon and Sisar detachment faults, based on mapping with industry seismic reflection data [*Sorlien et al.,* 2016], well data, relocated seismicity and depth-converting fault time grids using the Harvard CVM-H 3D velocity model [*Nicholson et al.,* 2016].

Evaluation of CFM Fault Set, Proposed 2D Fold Models, and Alternative Fault Representations.

In addition to expanding the 3D CFM fault set for southern California and related issues of fault model completion, depth conversion, and extending faults deeper with relocated seismicity, there are also issues regarding fault model *evaluation* and *validation,* and how to properly discriminate between various competing alternative representations. For example, as previously mentioned, there is still a major on-going controversy regarding the faults responsible for the large vertical uplift events found at Pitas Point [*Rockwell et al.,* 2014, 2016]. One model postulates that these uplift events are driven exclusively by slip on the N-dipping Pitas Point-Ventura fault (PPVF), that the size of the uplift events is characteristic of the average slip over the whole fault during rupture—yielding the prospect of multiple Holocene M7.7-M8 earthquakes on the PPVF, and that the PPVF exhibits a distinctive ramp-flat-ramp geometry, with the flat at 7 km depth (**Fig.3**)[*Hubbard et al.,* 2014; *Rockwell et al.,* 2016]. The alternative model considers the uplift events at Pitas Point to be anomalous and localized, and therefore not representative of the average slip at depth further along strike; to consider the PPVF—and the Red Mountain fault with which it merges—to be relatively steep without a flat detachment, and that the uplift at Pitas Point is primarily driven by slip on the S-dipping Padre Juan fault, its interaction with the PPVF, or the result of a localized restraining bend or possible secondary tear fault [*Nicholson et al.,* 2016].

Figure 15 (*right*) shows these two alternative fault models in CFM for the combined Pitas Point-Red Mountain fault. The dark-blue, ramp-flat-ramp model [*Hubbard et al,* 2014] is based on limited well data in the onshore Ventura basin and a 2D fold model (**Fig.12**, bottom) that has been projected offshore. It is the fault geometry assumed for proposed M7.7-M8 earthquakes on the Pitas Point-Ventura fault [*Ryan et al.,* 2015; *Rockwell et al.,* 2016]. The red-purple, more steeply dipping model is based mostly on the offshore mapping with industry MCS data (**Figs.4-6**), and combining this with relocated seismicity (1981-2012) in the eastern Santa Barbara Channel [*Nicholson and Kamerling,* 1998; *Kamerling et al.,* 2003; *Nicholson et al,* 2014; 2015]. To evaluate the validity of these two alternative fault models, we can compare them with *independent* datasets of relocated hypocenters for the 1978 M5.9 Santa Barbara and 2013 M4.8 Isla Vista earthquakes. These are the two largest reasonably recorded events in the area and are data not previously included in either model construction. If we do so, this indicates that the steeply dipping fault model, rather than the alternative ramp-flat model, is more consistent with this recent distribution of earthquakes and slip at depth.

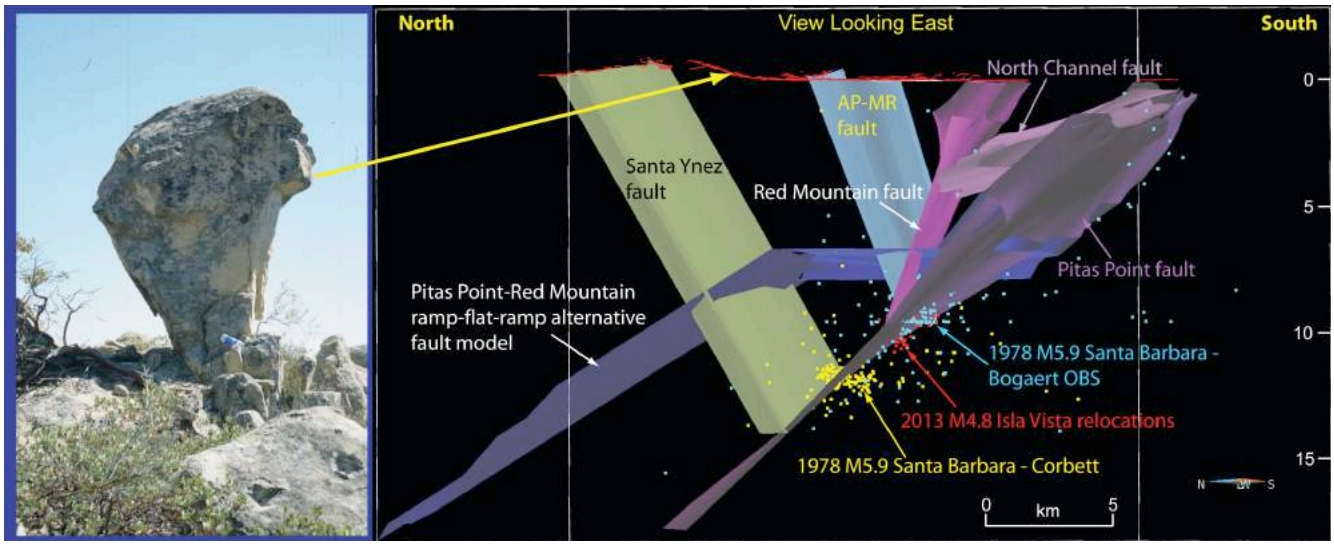

Figure 15. (*left*) Example of Precariously Balanced Rocks present in the foothills behind Santa Barbara and directly above ramp-flat fault source model assumed for proposed Holocene M8 earthquakes [*Brune,* 2009]. (*right*) Oblique 3D view looking East of North Channel-Pitas Point-Red Mountain fault system (red-purple) [*Nicholson et al.,* 2015] and alternative ramp-flat Pitas Point-Red Mountain fault model (dark blue)[*Hubbard et al.,* 2014]. Independent datasets of relocated hypocenters for the 1978 M5.9 Santa Barbara and 2013 M4.8 Isla Vista earthquakes (not included in either original model construction) indicate that the steeply dipping fault model (red-purple) is more consistent with this recent slip than the proposed alternative ramp-flat model (dark blue)[*Nicholson et al.,* 2016].

Other *independent* data also suggest that the proposed ramp-flat-ramp model for the Pitas Point-Ventura fault (PPVF) is not correct and that it is unlikely that the large uplift events at Pitas Point are indicative of ~M8 earthquakes in the Santa Barbara-Ventura area. First, there is a line of Precariously Balanced Rocks in the foothills above Santa Barbara and Montecito (**Fig.15**, *left*)[*Brune,* 2009]. The presence, age and fragility of these rocks generally preclude the occurrence of shallow Holocene M8 earthquakes on the PPVF regardless of which fault geometry is assumed at depth. Second, the distinct lack of surface fault rupture onshore, or seafloor offset offshore for the blind PPVF, the lack of consistency in uplift events spaced just 15 km apart [*McAuliffe et al.,* 2015], plus the distinct lack of widespread tsunami deposits [*Reynolds et al.,* 2015] that would be expected from such shallow (<15 km) M8 earthquakes that extend ten's of km offshore also indicate that the proposed multiple Holocene earthquakes responsible for the uplift were unlikely to be near M8 [*Nicholson et al.,* 2015; 2016]. Third, the actual subsurface 3D fault and fold geometry as drilled and imaged at Pitas Point or farther offshore (*e.g.,* **Figs.6&11**), the lack of any direct evidence for a presumed flat, horizontal detachment at 7 km, plus the known rates of footwall 3D basin subsidence and deformation [*Sorlien and Kamerling,* 2000; *Nicholson et al.,* 2007], demonstrate that: 1) the 2D ramp-flat-ramp model for the PPVF [*Hubbard et al.,* 2014] is not correct, 2) the assumptions used to construct the 2D model are not valid, and 3) to all extent and purposes, the presumed flat horizontal detachment for the PPVF at 7 km depth does not exist.

In terms of regional seismic hazard, it is also important to better resolve the depth extent of faults that may be the sources for proposed large earthquakes, what linkages may exist at depth between major fault systems, and whether major faults may (or may not) be detached at some shallow (7 km)[*Hubbard et al.,* 2014], mid-crustal (10-12 km)[*Levy and Rockwell,* 2015] or deeper structural level. To investigate these issues and to further help discriminate between alternative fault representations, the distribution of deep relocated seismicity (>15 km) was compared with specific predictions made by the different fault models for the PPVF. For example, one prominent prediction of the 2D ramp-flat-ramp fault model for the PPVF (**Fig.3**, *left*) is that owing to the presumed flat detachment, the deep Pitas Point-Red Mountain and San Cayetano faults are not significantly offset and fairly continuous at depth [*Hubbard et al.*, 2014], whereas in the more steeply dipping representation without the flat detachment (**Fig.3**, *right*), the two fault systems at depth retain their observed surface offset (**Fig.16**)[*Nicholson,* 2016].

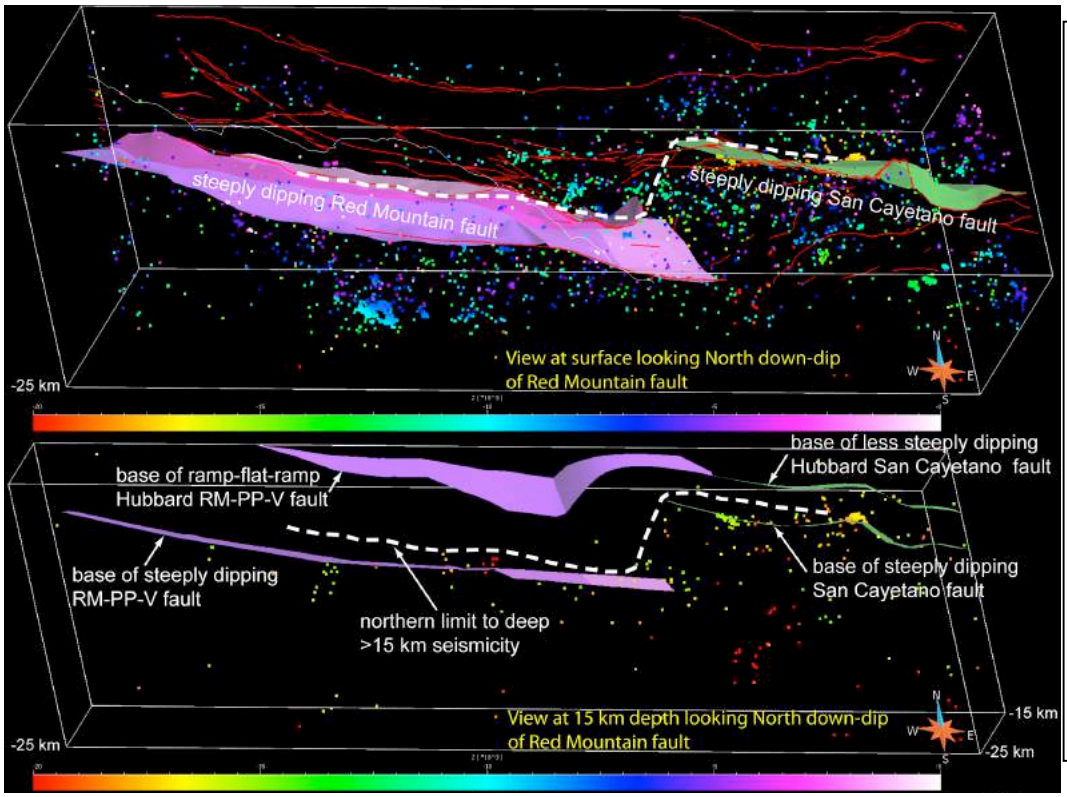

Figure 16. (*top*) Oblique 3D view looking down-dip from Red Mountain fault surface trace. White dashed line shows 10-km step north along strike to the San Cayetano fault. (*bottom*) Same down-dip view but starting at 15 km depth. The marked northern limit of deep seismicity (>15 km) shows the same 10-km step to the north. Also shown are alternative ramp-flat-ramp and less steeply dipping models for Red Mountain-Pitas Point-Ventura (RM-PP-V) and San Cayetano faults from *Hubbard et al.* [2014] which are inconsistent with this distribution of seismicity at depth.

Figure 16 is a rotated oblique 3D view looking down-dip (in the plane of slip) of the Red Mountain fault of the relocated seismicity and the alternative models in CFM for the San Cayetano (green) and Red Mountain-Pitas Point-Ventura (purple) faults [*Nicholson,* 2016]. At the surface (**Fig.16**, *top*), the RMF steps north along strike to the San Cayetano fault (white dashed line). If the fault is detached at some lower structural level [*Hubbard et al.,* 2014], this step north would not be expected to continue to deeper depths. However, looking only at seismicity deeper than 15 km (**Fig.16,** *bottom*), deeper than any proposed detachment level (7-12 km), there is a marked northern limit to this deep seismicity. This northern limit has the same step to the north as observed with the surface fault traces, indicating that this step in fault geometry and thus the faults themselves continue at relatively constant dip to depths of 18-20 km. The less steeply dipping or 2D ramp-flat-ramp fault models proposed by *Hubbard et al.* [2014] (that would project to be farther north at depth; **Fig.16,** *bottom*) are not consistent with this observation of a persistent step to the north in both the faults and related deep seismicity (white dashed line).

Localized Uplift at Pitas Point and Restraining Bend in the Pitas Point-Ventura Fault

A primary observation is that the size and number of individual uplift events, total uplift, and uplift rate found at Pitas Point since ~7 ka [*Rockwell et al.,* 2016] seems to be both localized and anomalous (**Fig.17**)[*Nicholson et al.,* 2016], and as such it is not indicative of either the fault slip expected farther along strike, or the average slip expected during large earthquake ruptures. Along most of the offshore Pitas Point fault, the fault exhibits no shallow near-seafloor fault offset since ~500 ka (**Figs.4&6**). High-resolution MCS data located 10 km or more west of Pitas Point also indicate that shallow, post-LGM sediments are not deformed at the blind Pitas Point fault. This lack of shallow fault offset compares with a predicted seafloor offset of ~10-12 m from just one large dynamic rupture event on this fault (**Fig.7**, *inset*)[*Ryan et al.,* 2015]. *Rockwell et al.* [2016] infer four such M7.7 to M8 fault rupture events since 6.7 ka, or an expected fault offset of the LGM unconformity of at least 50 m, if these proposed ~M8 events all occurred on the PPVF. Farther east onshore, *McAuliffe et al.* [2015] found only two (not four) ~5-6-m uplift events on the blind Ventura fault since about 9 ka, or an average uplift rate of ~1.6 mm/yr and an inferred fault slip rate of ~2.3 mm/yr. This is similar to the reverse slip rate for the Ventura fault from geodetic strain modeling [*Marshall et al.,* 2013] and the slip rate estimated for the offshore fault near the coast from folding above the blind fault tip [*Johnson et al.,* 2017]. Given the depth and dip of the Ventura fault beneath Pitas Point (**Fig.11**), however, the expected slip rate needed to match or produce the uplift rate at Pitas Point would be more on the order of about 8-9 mm/yr (*e.g.,* **Fig.17**).

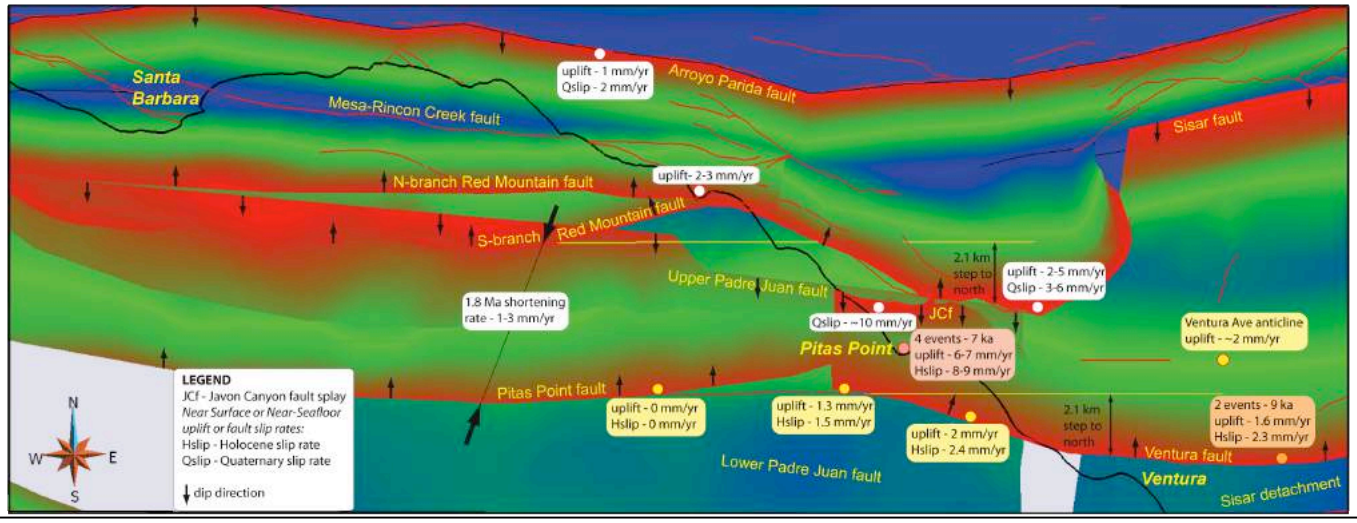

Figure 17. Uplift and inferred fault slip rates at Pitas Point (red) [*Rockwell et al,* 2016] are anomalous, and are not consistent with the number of uplift events or uplift rate found farther along strike onshore (orange) [*McAuliffe et al.,* 2015], the uplift & fault slip rates at or above the blind Pitas Point-Ventura fault (yellow) found offshore [*Johnson et al.,* 2016], or the uplift rate for Ventura Avenue anticline [*Sylvester,* 2000; *Marshall et al.,* 2013] and marine terraces found elsewhere along the coast [*Gurrola et al,* 2014; *Fredrickson,* 2016]. Pitas Point-Ventura and Red Mountain faults step ~2.1 km north at the coast, producing a restraining bend and enhanced, localized uplift in these left-oblique fault systems.

The uplift rate at Pitas Point (6-7 mm/yr) is also anomalous in comparison with other coastal uplift rates in adjacent areas (1-2 mm/yr)[*Gurrola et al.,* 2003; *Fredrickson,* 2016], and with the longer-term rate of vertical deformation and shortening derived from surface deformation modeling of the deformed top-Lower Pico horizon across the offshore North Channel-Pitas Point-Red Mountain fault system (1-3 mm/yr)[*Sorlien and Kamerling,* 2000]. The geodetic uplift rate of the Ventura Avenue anticline itself—which is supposedly driving the uplift at Pitas Point—is also only ~2 mm/yr [*Sylvester,* 2000; *Marshall et al.,* 2013, 2014]. This suggests that something else (an additional active fault or structural anomaly) is causing or contributing to this enhanced, localized uplift and the anomalous uplift events at Pitas Point.

At Pitas Point, besides to the N-dipping Ventura fault and Ventura Avenue anticline, there is also the S-dipping Padre Juan fault and N-verging San Miguelito anticline. The Padre Juan is an out-of-syncline thrust fault capable of generating anomalously large displacements for its size. In addition, at Pitas Point, both the onshore Ventura fault and Ventura Avenue anticline step over 2 km north to the offshore Pitas Point fault and Rincon anticline (**Fig.17**). This step north between the onshore and offshore structures may be in response to a hidden tear-fault or cross-fault at depth. Regardless, this creates a localized restraining bend in the left-oblique-reverse PPVF, and may further help explain why the uplift and uplift rate at Pitas Point is so anomalous. If so, then the uplift events found at Pitas Point, and the associated fault slip needed at depth, are not indicative of either the expected slip further along strike of the PPVF, or the average slip expected at depth during large earthquakes. Rather, this uplift at Pitas Point is probably localized to the restraining bend, where slip on the Padre Juan fault potentially predominates, or where the Padre Juan and PPVF strongly interact, which limits the length and depth of possible seismic ruptures and the earthquake and tsunami potential of the active fault(s) involved.

SUMMARY AND IMPLICATIONS FOR EARTHQUAKE & TSUNAMI HAZARDS

The high uplift rates of raised marine terraces observed at Pitas Point are anomalous. The uplift rates found at Pitas Point (6-7 mm/yr)[*Rockwell et al.,* 2016] are not continued farther west along the Santa Barbara-Ventura coast (2 mm/yr)[*Gurrola et al.,* 2014], and are not observed to the east for the Ventura Avenue anticline itself, where recent geodetic data [*Sylvester,* 2000] indicate an average uplift rate of ~2 mm/yr. The uplift rate at the blind Ventura fault is ~1.6 mm/yr [*McAuliffe et al.,* 2015]. The high inferred shortening rates at Pitas Point are not observed farther west offshore where the shortening rate measured across the Pitas Point fault to the S-branch of the Red Mountain fault is ~3 mm/yr [*Sorlien & Kamerling,* 2000]. At the coast, Holocene uplift rates inferred for the offshore Pitas Point fault from local folding above the blind fault tip are about ~2-2.3 mm/yr [*Johnson et al.,* 2017], but this folding and shallow slip decrease westward owing to increasing fault tip depth and decreasing regional shortening.

At Pitas Point, there is not one but two anticlinal folds: the upper N-verging, asymmetric San Miguelito anticline in the hanging wall of the S-dipping, listric Padre Juan fault, and the distinctly separate lower Ventura Avenue-Rincon anticline in its footwall [*Grigsby,* 1988]. Neither the N-verging fold, nor the Padre Juan fault are represented in the 2D fold model [*Hubbard et al.,* 2014] or in the subsequently derived rupture or earthquake and tsunami hazard models [*e.g., Ryan et al.,* 2015].

S-dipping, listric Padre Juan fault is independently late-Quaternary active. The fault exhibits 2.6 km of dip separation and much of this slip occurred since ~250 ka during Ventura Avenue fold growth [*Grigsby,* 1988]. Because emplacement of the San Miguelito fold was syntectonic with Ventura Avenue folding and would involve moving material from the footwall to the hanging-wall of the Ventura fault, this slip must have occurred while the Padre Juan fault acted independently. Both high-resolution and deep-penetration MCS reflection data indicate continued folding, progressive limb rotation and tilting in the footwall and hanging wall of the Pitas Point fault, indicating that both the S-dipping Padre Juan and N-dipping Pitas Point faults are still late-Quaternary active. The Padre Juan fault soles into the weak Rincon Shale at ~7 km depth, indicating it may exhibit large out-of-syncline thrust displacements.

Both the offshore Pitas Point fault and onshore Ventura fault are blind. Within the resolution of the seismic reflection data, the Pitas Point fault has not exhibited near-seafloor fault rupture in most places since 500 ka, although its hanging-wall does exhibit progressive limb rotation and tilting [*Sorlien et al.,* 2015] indicating that fault slip diminishes updip. The large seafloor offsets [*Ryan et al.,* 2015] and

widespread tsunami deposits expected from the proposed multiple, shallow ~M8 earthquakes on the Pitas Point-Ventura fault [*Rockwell et al.,* 2016] are not observed. Globally, the 10-12-m of fault slip at 2.5 km depth needed to explain the 8-11-m uplift events at Pitas Point always produces surface rupture.

Pitas Point-Ventura fault exhibits a restraining bend at Pitas Point. The onshore Ventura fault steps ~2.1 km north to the offshore Pitas Point fault. The Pitas Point-Ventura fault exhibits left-oblique fault slip. This change in fault geometry along strike creates a restraining bend of enhanced, localized uplift that is not representative of the uplift expected elsewhere along strike. This reinforces the idea that the uplift at Pitas Point is anomalous, whether it is from the Pitas Point fault, the Padre Juan fault, or some combination of the two, or even a possible tear fault that may be responsible for the restraining bend.

Implications for Earthquake and Tsunami Hazards

Fundamental questions regarding the nature of the subsurface structures driving coastal uplift, surface deformation, and related seismic and tsunami hazards include: What is the geometry of the principal fault(s) and fault-related fold(s) responsible for the coastal uplift at Pitas Point? How deep do these faults extend? Is this the N-dipping Pitas Point-Ventura fault that joins the Red Mountain fault to extend to depths of 20 km? Or is this the S-dipping, listric Padre Juan-Javon Canyon fault that only extends to a depth of 7 km? How do these two mutually cross-cutting faults interact and how do they affect the development of both N-verging and S-verging folds? What predictions do the current fault models make in terms of coastal uplift, fold development, fault slip, or potential seafloor offset [*Hubbard et al.,* 2014; *Ryan et al.,* 2015] and how do these model predictions compare with observed 3D fault and fold geometry [*Nicholson et al.,* 2015], and with measured rates of surface or seafloor deformation and geodetic strain [*Sorlien and Kamerling,* 2000; *Johnson et al.,* 2013; *Marshall et al.,* 2013], or compare with alternative interpretations that allow for or include S-dipping faults, like the Padre Juan fault? Do the large uplift events observed at Pitas Point [*Rockwell et al.,* 2014] reflect the average slip at depth on regional faults during presumed ~M8 earthquakes, or can these uplift events and the high rates of related anticlinal folding be considered—in many ways—anomalous, and likely the result of local space problems, like a local restraining bend or other possible secondary pattern of crustal deformation? Should we be considering that the high rates of coastal uplift at Pitas Point are not solely from fault slip on either exclusively N-dipping or S-dipping faults, but rather the result of the complex interaction between these two oppositely dipping fault sets?

In considering the seismic and tsunami hazard implications of the observed coastal uplift at Pitas Point, it is thus fundamentally important to determine what the basic geometry is of the fault or faults responsible for the uplift. If the uplift is occurring exclusively on the N-dipping Pitas Point-Ventura fault, as proposed by *Hubbard et al.* [2014], *Rockwell et al.* [2016] and as modeled by *Ryan et al.* [2015], then large uplift events at Pitas Point would be expected to correspond with even larger slip events at depth on the fault, as well as large surface offsets onshore, large uplift and 10-12-m seafloor offsets offshore (**Fig.7**, *inset*), and thus large seismic and tsunami amplitudes from Santa Barbara to Ventura [*Ryan et al,* 2015]. However, these expected and predicted large surface and seafloor fault offsets and related tsunami deposits are not observed. If instead the uplift is the result of slip at depth on the Ventura fault, but reflected at shallow levels as slip on the upper Padre Juan fault acting as a backthrust, then this uplift would be associated with additional uplift directed onshore, closer to the Javon Canyon fault. Again, large Holocene offsets on the Javon Canyon fault are not observed, but much of this Padre Juan fault slip could go into increased distributed blind subsurface folding at depth.

Alternatively, if the uplift at Pitas Point is the result of local space problems and largely driven by slip on the listric, S-dipping, out-of-syncline Padre Juan thrust fault that only extends to a depth of ~7 km, then uplift at Pitas Point would be again mainly associated with additional uplift directed onshore, or reflected as shallow slip on the onshore Ventura fault acting as a backthrust, and not associated with large seafloor displacements offshore. In addition, fault slip and folding would likely be confined to the upper 6-7 km, and mainly to weak bedding planes in the Rincon and other shale layers, limiting the down-dip seismogenic width of the fault rupture and potential stress drop, all of which would likely reduce the seismic and tsunami hazards estimated for this potential earthquake.

Of course, this does not mean to say that the North Channel-Pitas Point-Red Mountain fault system does not represent a significant seismic hazard, or that it could not link up with other faults to produce even larger damaging earthquakes. It certainly does represent a significant hazard and it potentially can link up with other faults to produce larger earthquakes. This N-dipping fault system already produced the damaging 1925 M6.8 and 1978 M5.9 Santa Barbara earthquakes, and given its mapped length and downdip width, it is quite capable of producing earthquakes greater than M7.2 [*Archuleta et al.,* 1997; *Kamerling et al.,* 2003; *Field et al.,* 2013]. It is just critically important to resolve the exact nature of the hazard and fault slip reflected by the observed coastal uplift pattern. However, it should be noted that the prominent step north from the Red Mountain fault to the San Cayetano fault (**Fig.16**) is maintained in the seismicity to depths of 18-20 km, indicating that dynamic rupture is unlikely to as readily propagate between these major fault systems at depth as proposed by *Hubbard et al.* [2014].

The major point is that the size, number and frequency of uplift events found at Pitas Point [*Rockwell et al.,* 2016] is highly unusual, very localized and anomalous. The four 8-11-m inferred Holocene uplift events since 6.7 ka are not repeated on the Ventura fault farther east [*McAuliffe et al.,* 2015], nor are they observed offshore on the Pitas Point-Ventura fault directly south of or farther west of Pitas Point [*Johnson et al.,* 2017]. Such 8-m uplift events, if produced by proposed ~M8 earthquakes and large 10-12-m slip events on a N-dipping Pitas Point-Ventura fault at 3 km depth beneath Pitas Point (**Fig.11**) would be expected to necessarily produce large onshore surface rupture and large offshore seafloor fault rupture, and evidence of similar discrete uplift events for 50-80 km along strike. The marked absence of this evidence farther along strike to the east or west indicates that the uplift at Pitas Point is not the result of ~M8 earthquakes, or necessarily slip on exclusively the N-dipping Pitas Point-Ventura fault. Rather these uplift events are related to something local to Pitas Point. The first-order characteristics that distinguish Pitas Point as anomalous are: 1) a major restraining bend in the left-oblique Pitas Point-Ventura fault, which would tend to enhance localized uplift (as is observed); and 2) the presence of the dominant-displacement, listric, S-dipping Padre Juan fault, which already exhibits a late-Quaternary fault slip rate capable of producing the uplift at Pitas Point. Explanations for the uplift at Pitas Point should then be focused on finding elusive evidence for four proposed ~M8 Holocene earthquakes, but rather how the complex interaction between oppositely dipping faults and the resulting complex 3D fault and fold geometry can generate such anomalous, localized uplift.

PRODUCTS AND DATA AVAILABILITY

Marine MCS reflection data, including 3D seismic surveys and 2D grids of both deep-penetration and high-resolution seismic data, are available from the USGS NAMSS web site [*Hart and Childs*, 2005](https://walrus.wr.usgs.gov/NAMSS/). Relocated earthquake hypocenter and revised focal mechanism catalogs are available from the SCEC Data Center (http://scedc.caltech.edu/eq-catalogs/) [*Hauksson et al.,* 2012 + updates; *Yang et al.,* 2012]. Offshore and onshore industry well logs and other well information are available from Bureau of Ocean Energy Management (BOEM) and Division of Oil, Gas & Geothermal Resources (DOGGR) (http://www.conservation.ca.gov/dog/Pages/Wellfinder.aspx). These industry datasets have been used to develop numerous subsurface structure maps and correlation cross sections [*e.g., Grigsby,* 1988; *Yeats et al.,* 1988; *Hopps et al.,* 1992; *Redin et al.,* 2005]. Many of the onshore maps and cross sections are available on-line at UCSB (https://projects.eri.ucsb.edu/hopps/). All products developed by this project, which primarily consist of new or updated digital 3D fault models are incorporated into the SCEC CFM Versions 5.1 [*Nicholson,* 2016; *Plesch et al.,* 2016] and 5.2 [*Nicholson et al.,* 2017] and its associated CFM fault database. This dataset is readily accessible on-line at: https://scec.usc.edu/scecpedia/CFM. Results were also presented at several national and international meetings [*Nicholson,* 2016; *Nicholson et al.,* 2016, 2017; *Plesch et al.,* 2016; *Sorlien et al.,* 2016] and are being finalized for publication in a suitable peer-reviewed journal.

PROJECT REPORTS, PUBLICATIONS, AND RELATED PRESENTATIONS

Behl, R.J., C. Nicholson, C.C. Sorlien, J.P. Kennett, C. Marshall, S.H. Decesari and D.E. Escobedo. Chrono-stratigraphy of the Quaternary Santa Barbara Basin: An integrated geophysical, sedimentologic and paleoceano-graphic approach, *2016 AAPG Pacific-Rocky Mountain Joint Meeting Program*, p.39, Las Vegas, NV (2016).

DeHoogh, G.L., C.C. Sorlien, C. Nicholson, C.S. Schindler and R.D. Francis, Structure, Evolution and Tectonic Significance of the Eastern Boundary of the Outer Continental Borderland, *SEPM Gorsline Special Publication*, accepted, 14 pp (2017).

Nicholson, C., 3D Fault Geometry & Slip History of the North Channel-Pitas Point-Red Mountain Fault System, SCEC Ventura SFSA workshop, *2016 SCEC Annual Meeting Proceedings & Abstracts*, **XXVI**, p.113 (2016).

Nicholson, C., A. Plesch and J.H. Shaw, Community Fault Model Version 5.2: Updating & expanding the CFM 3D fault set and its associated fault database, *2017 SCEC Annual Meeting Proceedings & Abstracts*, **XXVII**, poster 234, p.142-143 (2017).

Nicholson, C., C.C Sorlien and T.E. Hopps, Anomalous Uplift at Pitas Point: Implications from Onshore & Offshore 3D Fault & Fold Geometry and Observed Fault Slip, *2016 SCEC Annual Meeting Proceedings & Abstracts*, **XXVI**, poster 006, p.216-217 (2016).

Nicholson, C., C.C Sorlien, T.E. Hopps and M.J. Kamerling, Anomalous Uplift at Pitas Point: Localized Phenomena or Indicator of Tsunamigenic M8 Earthquakes Along Coastal California?, *Eos (Transactions of AGU)*, **97** (52), Abstract OS21A-1935 (2016).

Plesch, A., C. Nicholson, C. Sorlien, J.H. Shaw and E. Hauksson, CFM Version 5.1: New and revised 3D fault representations and an improved database, *2016 SCEC Annual Meeting Proceedings & Abstracts*, **XXVI**, poster 003, p.222-223 (2016).

Sorlien, C.C, C. Nicholson, R.J. Behl and M.J. Kamerling, Displacement direction and 3D geometry for the south-directed North Channel–Pitas Point fault system and north-directed ramps, decollements, and other faults beneath Santa Barbara Channel, *2016 SCEC Annual Meeting Proceedings & Abstracts*, **XXVI**, poster 007, p.238-239 (2016).

REFERENCES

Archuleta, R.J., C. Nicholson, J. Steidl, L. Gurrola, C. Alex, E. Cochran, G. Ely and T. Tyler, Initial Source and Site Characterization Studies for the UC Santa Barbara Campus, Report on the UC/CLC Campus Earthquake Program, *LLNL Report UCRL-ID-129196*, 83 pp. (1997).

Bogaert, B., An aftershock study of the Santa Barbara earthquake of August 13, 1978, *M.S. Thesis*, University of California, Santa Barbara, 55 pp., 1984.

Brune, J., *SCEC Precarious Rock and Related Archive*, Santa Ynez Range, 2009.

Bryant, W. A. (compiler), 2005, Digital Database of Quaternary and Younger Faults from the Fault Activity Map of California, version 2.0: accessed July 2010 from California Geological Survey Web Page, http://www.consrv.ca.gov/cgs/information/publications/Pages/QuaternaryFaults_ver2.aspx.

Burdick, D. J., and W.C. Richmond, (1982), A summary of geologic hazards for proposed OCS oil and gas lease sale 68, Southern California, MMS and USGS Open-File Report 82-33

Dolan, J.F., J.H. Shaw and T.K. Rockwell, The Ventura Region Special Fault Study Area: Towards an understanding of the potential for large, multi-segment thrust ruptures in the Transverse Ranges, *2012 SCEC Annual Meeting Proc. & Abstracts*, **XXII**, p.99-100 (2012).

Dunham, E.M., D. Belanger, L. Cong and J.E. Kozdon, Earthquake ruptures with strongly rate-weakening friction and off-fault plasticity, Part 2: nonplanar faults, *Bull. Seismol. Soc. Am.,* **101**, n.5, p. 2308-2322 (2011).

Field, E.H., G.P. Biasi, P. Bird, et al., 2013, Uniform California earthquake rupture forecast, v.3 (UCERF3)—The time-independent model, *USGS Open-File Report 2013–1165*, 97 p., http://pubs.usgs.gov/of/2013/1165.

Fisher, M.A., W.R. Normark, H.G. Greene, H.J. Lee and R.W. Sliter, Geology and tsunamigenic potential of submarine landslides in Santa Barbara Channel, Southern California, *Marine Geology*, **224**, p.1-22 (2005).

Fredrickson, S.M., The geomorphic transition between the Santa Barbara and Ventura fold belts near Rincon Point, California, *M.S. Thesis*, University of California, Santa Barbara, 114 pp. (2016).

Grigsby, F.B., 1986, Quaternary tectonics of the Rincon and San Miguelito oil fields area, western Ventura basin, California, M.S. thesis, 110 pages, Oregon State University, Corvallis.

Grigsby, F.B., Structural development and the Ventura Avenue anticlinal trend at the San Miguelito and Rincon oil fields, Ventura County, California, in *Santa Barbara and Ventura Basins: Tectonics, Structure, Sedimentation, Oilfields Along an East-West Transect,* A.G Sylvester and G.C. Brown, eds., *Coast Geological Survey Guidebook 64*, p. 111-124 (1988).

Gratier, J.-P., Hopps, T., Sorlien, C. C., and Wright, T., 1999 Recent crustal deformation in southern California deduced from the restoration of folded and faulted strata, *J. Geophys. Res.,* **v. 104**, p. 4887-4899

Gurrola, L.D., E.A. Keller, J.H. Chen, L.A. Owen and J.Q. Spencer, Tectonic geomorphoogy of marine terraces: Santa Barbara fold belt, California, *Geol. Soc. Am. Bulletin*, **126,** n.1/2, p.219-233 (2014).

Hart, P. E., and J. R. Childs (2005), National archive of marine seismic surveys (NAMSS): Status report on U.S. Geological Survey program providing access to proprietary data, *Eos Trans. AGU*, **86**, Abstract S41A-10.

Hauksson, E., C. Nicholson, J.H. Shaw, A. Plesch, P.M. Shearer, D.T. Sandwell and W. Yang, Refined views of strike-slip fault zones, seismicity, and state of stress associated with the Pacific-North America plate boundary in Southern California, *Eos (Transactions of AGU)*, **94** (52), Abstract T21E-05 (2013).

Hauksson, E., Understanding seismicity in the context of complex fault systems and crustal geophysics, *2012 SCEC Annual Meeting Proc. & Abstracts*, **XXII**, p.108 (2012).

Hauksson, E., W. Yang and P. Shearer, Waveform relocated earthquake catalog for Southern California (1981 to June 2011), *Bull. Seismol. Soc. Am.,* **v.102,** n.4, p.2239-2238, doi:10.1785/0120110241, 2012.

Herbert, J. and M. Cooke, 2012, Sensitivity of the Southern San Andreas fault system to tectonic boundary conditions and fault configuration, *Bull. Seismol. Soc. Am.,* **102,** p.2046-2062, doi:10.1785/0120110316.

Herbert, J., The role of fault complexity and secondary faults on fault slip, *SCEC Special Fault Study Area Workshop on San Gorgonio Pass,* June, 2012.

Hopps, T.E., H.E. Stark, and R.J. Hindle, *Subsurface geology of Ventura Basin, California, Ventura Basin Study Group Report*, 45 pp., 17 structure contour maps and 84 structure panels comprising 21 cross sections, Rancho Energy Consultants, Inc., Santa Paula, CA, 1992.

Hopps, T.E., H.E. Stark, R.J. Hindle, J.H. Thompson, and G.C. Brown, CS30: Correlated section across Central Ventura Basin from T5N/R19W to T1N/R18W, California, *Pacific Section–Am. Assoc. Petrol. Geol. Cross Section*, April, 1995.

Hubbard, J., J.H. Shaw, J.F. Dolan, T.L. Pratt, L. McAuliffe and T. Rockwell, Structure and seismic hazard of the Ventura Avenue anticline and Ventura fault, California: Prospect for large, multisegment ruptures in the Western Transverse Ranges, *Bull. Seismol. Soc. Am.*, 104, n.3, doi:10.1785/0120130125 (2014).

Huftile, G. and R.S. Yeats, Convergence rates across a displacement transfer zone in the western Transverse Ranges, Ventura basin, California, *J. Geophys. Res.*, v. **100**, p. 2043–2068 (1995).

Iwerks, J., *Perspective view and geologic cross section of the Western Transverse Ranges, California.* Composite cross section department wall mural (7 m x 1.5 m) modified by C. Nicholson & J. Iwerks from mapping by M. Kamerling, T. Redin, C. Sorlien and T. Dibblee.

Johnson, S.Y., P. Dartnell, et al., California State Waters Map Series -- Offshore Ventura and Carpenteria, California, *USGS Scientific Investigations Maps 3254 & 3261*, http://pubs.usgs.gov/sim/3254/, 2013.

Johnson, S.Y., S.R. Hartwell, C.C. Sorlien, P. Dartnell and A.C. Ritchie, Latest Quaternary structural and stratigraphic controls on continental shelf morphology along a transpressive transform margin, Santa Barbara Channel, California, *Eos (Transactions of AGU)*, **97** (52), Abstract OS12B-01 (2016).

Johnson, S.Y., Hartwell, S.R., Sorlien, C.C., Dartnell, P., and Ritchie, A.C., Shelf evolution along a transpressive transform margin, Santa Barbara Channel, California, *Geosphere,* **13**, p. 1–37, doi:10.1130/GES01387.1 (2017).

Kamerling, M.J., C.C. Sorlien and C. Nicholson (2003), 3D development of an active oblique fault system, northern Santa Barbara Channel, California, *Seismol. Res. Lett.*, v. **74**, n.2, p. 248.

Kamerling, M.J., C.C. Sorlien, and C. Nicholson (1998), Subsurface faulting and folding onshore and offshore of Ventura basin: 3D map restoration across the Oak Ridge fault, *SCEC 1998 Annual Meeting Report,* p.68-69.

Lajoie, K.R., A.M. Sarna-Wojcicki and R.F. Yerkes, Quaternary chronology and rates of crustal deformtion in the Ventura area, California, in *Geol. Soc. Am. Cordilleran Section Guidebook*, p.43-51 (1982).

Levy, Y. and T.K. Rockwell, Structural Architecture of the Western Transverse Ranges and Potential for Large Earthquakes, *Eos (Transactions of AGU)*, **96** (52), Abstract T41A-2856 (2015).

Lozos, J.C. and D.D. Oglesby, Seemingly minor details of fault geometry may strongly affect rupture propagation, *Seismol. Res. Lett.,* **83**, n.2, p.370, 2012.

Lozos, J.C. D.D. Oglesby and J.N. Brune, The effects of fault stepovers on ground motion, *Bull. Seismol. Soc. Am.*, **103**, n.3, p.1922-1934 (2013).

Lozos, J.C. D.D. Oglesby, J.N. Brune and K.B. Olsen, Rupture and ground-motion models on the northern San Jacinto Fault, incorporating realistic complexity, *Bull. Seismol. Soc. Am.*, **105**, n.4, p.1931-1946 (2015).

Marshall, C.J., C. Sorlien, C. Nicholson, R.J. Behl and J.P. Kennett, Sedimentation in an active fold and thrust belt, Santa Barbara Basin, California: Local and regional influences on the spatial and temporal evolution of sedimentation from 1.0 Ma to Present, *AAPG National Meeting,* Long Beach, CA (2012).

Marshall, S.T., G.J. Funning and S.E. Owen, Fault slip rates and interseismic deformation in the western Transverse Ranges, California, *J. Geophys. Res,* **v.118**, p.4511-4534, doi:10.1002/jgrb.50312 (2013).

Marshall, S.T., G.J. Funning and S.E. Owen, The distribution of fault slip rates in the Ventura fault system, CA, *2014 SCEC Annual Meeting Proceedings & Abstracts*, **XXIII**, poster 093, p.161 (2014).

Marshall, S.T., M.L. Cooke and S.E. Owen, Interseismic deformation associated with three-dimensional faults in the greater Los Angeles region, California, *J. Geophys. Res.*, **114**, n.B12, B12403 (2009).

McAuliffe, L.J., J.F. Dolan, E.J. Rhodes, J. Hubbard, J.H. Shaw and T.L. Pratt, Paleoseismologic evidence for large-magnitude (Mw7.5–8.0) earthquakes on the Ventura blind thrust fault: Implications for multifault ruptures in the Transverse Ranges of southern California, *Geosphere*, **11**, no. 5, 1629–1650. (2015).

Nicholson, C., Continuing to build the SCEC 3D Community Fault Model, *2003 SCEC Annual Report,* n.03027, 5 pp. (2003).

Nicholson, C., Continuing to build and evaluate the SCEC 3D Community Fault Model, *2005 SCEC Annual Report*, n.05120, 6 pp. (2005).

Nicholson, C. and M.J. Kamerling, Reliability of 2D kinematic fold models to infer deep fault structure in the western Transverse Ranges, California, *Proceedings of the NEHRP Conference and Workshop on the Northridge, California Earthquake of January 17, 1994*, v. **II**, p. 299–306 (1998).

Nicholson, C., J. Kennett, C. Sorlien, S. Hopkins, R. Behl, et al., Santa Barbara Basin study extends global climate record, *Eos (Transactions of American Geophysical Union)*, **87**, n.21, p.205-208 (2006).

Nicholson, C., A. Plesch, C. Sorlien, J.H. Shaw and E. Hauksson, Updating the 3D fault set for the SCEC Community Fault Model (CFM-v4) and revising its associated fault database, *2013 SCEC Annual Meeting Proceedings & Abstracts*, **XXIII**, poster 123, p.134 (2013).

Nicholson, C., A. Plesch, C.C. Sorlien, J.H. Shaw and E. Hauksson, The SCEC 3D Community Fault Model (CFM Version 5.0): An updated and expanded fault set of oblique crustal deformation and complex fault interaction for southern California, *Eos (Transactions of AGU)*, **95** (52), Abstract T31B-4584 (2014).

Nicholson, C., A. Plesch, J. Shaw, E. Hauksson and P. Shearer, Improvements in SCEC Community Fault Model for Version 4.0, *UCERF-3 California Statewide Fault Model & Paleoseismic Workshop*, Pomona, CA (2011).

Nicholson, C., A. Plesch, J.H. Shaw and E. Hauksson, Upgrades and improvements to the SCEC Community Fault Model: Increasing 3D fault complexity and compliance with surface and subsurface data, *2012 SCEC Annual Meeting Proceedings & Abstracts*, **XXII**, p.125-126 (2012).

Nicholson, C., E. Hauksson, A. Plesch and P. Shearer, Resolving 3D fault geometry at depth along active strike-slip faults: Simple or complex?, *2008 SCEC Annual Meeting Proceedings & Abstracts*, **XVIII**, p.143-144 (2008).

Nicholson, C., M.J. Kamerling, C.C. Sorlien, T.E. Hopps and J.-P. Gratier, Subsidence, compaction and gravity-sliding: Implications for 3D geometry, dynamic rupture and seismic hazard of active basin-bounding faults in southern California, *Bulletin of the Seismological Society of America,* **97**, n.5, p.1607-1620 (2007).

Nicholson, C., Updating Active 3D Fault Geometry in Special Fault Study Areas and Improving the SCEC Community Fault Model (CFM), *2014 SCEC Annual Report*, n.14015, 8 pp (2015).

Nicholson, C., Continuing to Evaluate & Update Active 3D Fault Geometry in Special Fault Study Areas and to Improve the SCEC Community Fault Model, *2015 SCEC Annual Report*, n.15154, 9 pp (2016).

Nicholson, C., A. Plesch, C.C. Sorlien, J.H. Shaw and E. Hauksson, The SCEC Community Fault Model Version 5.0: An updated and expanded 3D fault set for southern California, *2015 Pacific Section AAPG Joint Meeting Program*, p.77, Oxnard, CA (2015).

Nicholson, C., C.C Sorlien, T.E. Hopps and A.G. Sylvester, Anomalous Uplift at Pitas Point, California: Whose fault is it anyway?, *2015 SCEC Annual Meeting Proceedings & Abstracts*, **XXV**, poster 221, p.171 (2015).

Niño,F., J. Chéry, and J.-P. Gratier, 1998, Mechanical modeling of compressional basins: Origin and interaction of faults, erosion, and subsidence in the Ventura basin, California, *Tectonics,* v.17, n.6, p. 955–972.

O'Connell, D., Earthquake locations, focal mechanisms, and GPS near Ventura, Western Transverse Ranges, California: The crust has a thick skin, *Eos (Trans. AGU),* **76,** n.46, p. F141 (1995).

Pacific Section-AAPG, *Pacific Petroleum Geology Newsletter*, cover+page 3, Nov-Dec (2014).

Plesch, A., C. Nicholson, C. Sorlien, J.H. Shaw and E. Hauksson, SCEC Community Fault Model Version 5.0, *2014 SCEC Annual Meeting Proceedings & Abstracts*, **XXIII**, poster 096, p.171 (2014).

Plesch, A., C. Nicholson, J.H. Shaw, E. Hauksson and P.M. Shearer, New developments for the SCEC Community Fault Model and its associated fault database, *2010 SCEC Annual Meeting Proceedings & Abstracts*, **XX**, p.261-262 (2010).

Plesch, A., J. Shaw et. al., Community Fault Model (CFM) for Southern California, *Bulletin of the Seismological Society of America*, **v.97**, n.6, p.1793–1802, doi: 10.1785/0120050211 (2007).

Redin, T., J. Forman and M.J. Kamerling, 1998, Regional structure cross section across the eastern Santa Barbara Channel, from eastern Santa Cruz Island to the Carpinteria area, Santa Ynez Mountains, in Kunitomi, D.S., Hopps, T.E., and Galloway, J.M., eds., *Structure and Petroleum Geology, Santa Barbara Channel, California*: Bakersfield, CA, *Pacific Section AAPG MP-46,* p. 195-197, plate 3.

Redin, T., J. Forman and M.J. Kamerling, 2005, Santa Barbara Channel structure and correlation sections, *Pacific Section AAPG Cross Sections CS-32 through CS-42*, Bakersfield, CA.

Reynolds, L.C. and A.R. Simms, Late Quaternary relative sea level in Southern California and Monterey Bay, *Quaternary Science Reviews,* **126,** p. 57-66 (2015).

Reynolds, L.C., Simms, A.R., Rockwell, T.K., Peters, R. (2015) Holocene Evolution of Carpinteria Marsh, Southern California: Storms and Subsidence. Poster Presentation, Southern California Earthquake Center Annual Meeting, Palm Springs, CA, Sept. 2015.

Richmond, W. C., Cummings, L. J., Hamlin, S., and Nagaty, M. E., 1981, Geologic hazards and constraints in the area of proposed OCS oil and gas lease sale 48, southern California: U. S. Geological Survey Open-File Report 81-307, 37 p

Rockwell, T. K., Keller, E. A., Dembroff, G. R., Quaternary rate of folding of the Ventura Avenue anticline, western Transverse Ranges, southern California, *Geol. Soc. Am. Bulletin*, **100**, p. 850-858 (1988).

Rockwell, T., K. Wilson, L. Gamble, M. Oskin, and E. Haaker, Great earthquakes in the western Transverse Rages of southern California on the Pitas Point-Ventura thrust system, *5th International INQUA Meeting on Paleoseismology, Active Tectonics and Archeoseismology (PATA)*, Busan, Korea (2014).

Rockwell, T., Large co-seismic uplift of coastal terraces across the Ventura Avenue Anticline: Implications for the size of earthquakes and the potential for tsunami generation, *2011 SCEC Annual Meeting Proceedings & Abstracts*, **XXI**, p.7, also *2nd INQUA-IGCP Conference on Paleoseismology,* Corinth , Greece (2011).

Rockwell, T.K., K. Clark, L. GAmble, M.E. Oskin, E.C. Haaker and G.L. Kennedy, Large Transverse Range earthquakes cause coastal upheaval near Ventura, Southern California, *Bulletin of the Seismological Society of America*, **v.106**, n.6, doi: 10.1785/0120150378, 14 pp (2016).

Ryan, K.J., E.L. Geist, M. Barall and D.D. Oglesby, Dynamic models of earthquakes and tsunamis from rupture on the Pitas Point and lower Red Mountain faults offshore Ventura, California, *Seismological Research Letters,* **86**, n.2b, p.666 (2015).

Sarna-Wojcicki, A.M., K.R. Lajoie and R.F. Yerkes (1987). Recurent Holocene displacement on the Javon Canyon fault—a comparison of fault-movement history with calculated average recurrence intervals, *USGS Professional Paper* **1339**, p.125-136 (1987).

Sarna-Wojcicki, A. M., K. M. Williams, and R. F. Yerkes (1976). Geology of the Ventura Fault, Ventura County, California, USGS Miscellaneous Field Studies, map MF-781, 3 sheets, scale 1:6000.

Sarna-Wojcicki, A. M., and R. F. Yerkes (1982). Comment on article by R. S. Yeats entitled "Low-shake faults of the Ventura Basin, California", in *Neotectonics in Southern California*, J. D. Cooper (Editor), Geological Society of America, 78th Cordilleran Section Annual Meeting, Guidebook, 17–19.

Shaw, J.H., A. Plesch, C. Tape, M.P. Suess, T. Jordan, G. Ely, E. Hauksson, J. Tromp, T. Tanimoto, R. Graves, K. Olsen, C. Nicholson *et al.*, Unified Structural Representation of the southern California crust and upper mantle, *Earth & Planetary Science Letters,* **415**, p.1-15, doi:10.1016/201501016 (2015).

Shi, Z., Dynamic rupture models along irregular faults, SCEC San Gorgonio Pass SFSA Workshop, *2014 SCEC Annual Meeting Proceedings & Abstracts*, **XXIII** (2014).

Shi, Z. and S.M. Day, Ground-motion simulations from 3D dynamic rupture simulations of dipping rough-fault events, *Seismological Research Letters,* **86,** n.2B, p.664, 2015

Shi, Z., S. Ma, S.M. Day and G.P. Ely, Dynamic rupture along the San Gorgonio Pass section of the San Andreas fault, *Seismol. Res. Lett.*, **83**, n.2, p. 423, 2012.

Sliter, R.W., Triezenberg, P.J., Hart, P.E., *et al.*, High-resolution chirp and mini-sparker seismic reflection data from the southern California continental shelf—Gaviota to Mugu Canyon: U.S. Geological Survey Open-File Report 2008–1246, available at http://pubs.usgs.gov/of/2008/1246/ (2008).

Sorlien, C. C., J. P. Gratier, B. P. Luyendyk, J. S. Hornafius, and T. E. Hopps, Map restoration of folded and faulted late Cenozoic strata across the Oak Ridge fault, onshore and offshore Ventura basin, California, *Geol. Soc. America Bull.*, **v. 112**, p. 1080-1090, 2000.

Sorlien, C.C, C. Nicholson, R.J. Behl, C.J. Marshall and J. Kennett, The Quaternary North Channel-Pitas Point Fault System in Northwest Santa Barbara Channel, California, *Eos (Transactions of AGU)*, **95** (52), Abstract T34A-07 (2014).

Sorlien, C.C, C.J. Marshall, C. Nicholson et al., Post-1 Ma deformation history of the anticline forelimb above the Pitas Point-North Channel fault in Santa Barbara Channel, California, *2012 SCEC Annual Meeting Proceedings & Abstracts*, **XXII**, p.139-140 (2012).

Sorlien, C.C. and M.J. Kamerling, 1998, Fault displacement and fold contraction estimated from unfolding of Quaternary strata onshore and offshore Ventura basin, California. *U.S. Geological Survey NEHRP Final Technical Report 97-GR-03085*, 16 pp., digital map scale 1/100,000.

Sorlien, C.C. and M.J. Kamerling, M. J., Fault displacement and fold contraction estimated by unfolding of Quaternary strata, onshore and offshore Ventura basin, California, *Final Technical Report to U.S. Geological Survey NEHRP*, contract 99HQGR0080 (2000).

Sorlien, C.C., J.T. Bennett, M.-H. Cormier, B.A. Campbell, C. Nicholson and R.L. Bauer, Late Miocene-Quaternary fault evolution and interaction in the Southern California Inner Continental Borderland, *Geosphere*, in press, 2015.

Sorlien, C.C. and C. Nicholson, Post-1 Ma deformation history of the Pitas Point-North Channel-Red Mountain fault system and associated folds in Santa Barbara Channel, California, *USGS Final Technical Report,* Award G14AP00012, 24 pp. (2015).

Sorlien, C.C, C. Nicholson, M.J. Kamerling and R.J. Behl, Strike-slip displacement on gently-dipping parts of the Hosgri fault and fold-related relief growth patterns above the blind oblique-slip North Channel-Pitas Point-Red Mountain fault system, *2015 SCEC Annual Meeting Proceedings & Abstracts*, **XXV**, poster 220, p.185 (2015).

Sylvester, A.G. and J. Heinemann, Preseismic tilt and triggered reverse faulting due to unloading in a diatomite quarry near Lompoc, California, *Seismological Research Letters,* **67,** n.6, p.11-18 (1996).

Sylvester, A.G., Aseismic growth of Ventura Avenue anticline (1978 to 1991): Evidence of aneslastic strain release in Ventura basin, southern California, *Eos (Transaction of AGU)*, **76**, p.F141 (1995).

Sylvester, A.G., Aseismic growth of Ventura Avenue anticline, Southern California, 1978 to 1997: Evidence from precise leveling, *Surveying and Land Information Systems,* **60***,* No.2, pp. 95-108 (2000).

Tarnowski, J.M. and D.D. Oglesby, Dynamic models of potential earthquakes in the San Gorgonio Pass, CA, *Eos (Transactions of AGU)*, **93** (52), Abstract S21B-2519 (2012).

Teran, O.J., J.M. Fletcher, T.R. Rockwell, K.W. Hudnut, M.E. Oskin, et al., Structural controls on the surface rupture associated with the M7.2 El Mayor-Cucapah earthquake: A comparative analysis of scarp array kinematics, orientation, lithology and width, *2011 SCEC Annual Meeting,* **XXI**, p. 236-237 (2011).

Thibert, B., J.-P. Gratier and J.-M. Morvan, A direct method for modeling and unfolding developable surfaces and its application to the Ventura Basin (California), *Journal of Structural Geology*, **v. 27**, p.303-316, 2005.

Trugman, D.T., and E.M. Dunham, A 2D pseudo-dynamic rupture model generator for earthquakes on geometrically complex faults, *2013 SCEC Annual Meeting Proceedings & Abstracts*, **XXIII**, p.151 (2013).

U.S. Geological Survey and California Geological Survey, 2006, Quaternary fault and fold database for the United States, accessed July 2010 from USGS web site: http://earthquake.usgs.gov/hazards/qfaults/.

Yang, W., E. Hauksson and P. Shearer, Computing a large refined catalog of focal mechanisms for Southern California (1981–2010): Temporal stability of the style of faulting, *Bull. Seismol. Soc. Am.,* **v.102,** n.3, p.1179-1194, doi:10.1785/0120110311, 2012.

Yeats, R. S., Huftile, G. J., and Grigsby, F. B., 1988, Oak Ridge fault, Ventura fold belt, and the Sisar decollement, Ventura basin, California, *Geology*, **v. 16**, p. 1112-1116.

Yeats, R.S., 1981, Deformation of a 1 Ma Datum, Ventura Basin, California: U. S. Geological Survey, Technical Report, Contract No. 14-08-0001-18283.

Yeats, R.S., G.J. Huftile, and L.T. Sitt, Late Cenozoic tectonics of the east Ventura basin, California, *Am. Asoc. Petrol. Geol. Bull.,* **v. 78**, p.1040-1074, 1994.

Yeats, R.S., Huftile, G.J., and Grigsby, F.B., 1988, Oak Ridge fault, Ventura fold belt, and the Sisar decollement, Ventura basin, California, *Geology*, **v. 16**, p. 1112-1116.

Yeats, R.S., Large-scale Quaternary detachments of Ventura basin, southern California, *Journal of Geophysical Research,* **v. 88**, p.569-583 (1983).

Yeats, R.S., Late Quaternary slip rate on the Oak Ridge Fault, Transverse Ranges, California: Implications for seismic risk, *Journal of Geophysical Research*, v. **93**, p. 12,137-12,149, 1988.

Zhu, L. and H. Kanamori, Moho depth variation in Southern California from teleseismic receiver functions, *Journal of Geophysical Research,* **v.105**, n.2, p. 2969–2980, 2000.